REDUCTION IN SKELETAL MUSCLE CHLORIDE CONDUCTANCE IMPROVES CONTRACTILE FORCE IN WILDTYPE, BUT NOT IN HYPERKALEMIC PERIODIC PARALYSIS MICE

By

Amanda Higgins

A thesis submitted to the Faculty of Graduate and Post-Doctoral studies of the University of Ottawa

In partial fulfillment of the requirements of the Degree of

Masters of Science

Department of Cellular and Molecular Medicine

Faculty of Medicine

University of Ottawa

ABSTRACT

Hyperkalemic periodic paralysis (HEPP) is an inherited, autosomal disorder characterized by myotonia and periodic paralysis in skeletal muscle. The hallmark of the disease is a severe sensitivity to the K^+-induced force depression, the cause of the paralysis. Previous studies have provided evidence that the sensitivity to the K^+-induced force depression can be alleviated when the Cl^- conductance (G_{Cl}) is lowered. However, those studies were carried out at non-physiological temperatures (25°-30°C) and few stimulation frequencies. The overarching goal of this study was to examine whether manipulating G_{Cl} pharmacologically was a viable target for treating HEPP. This work sought to document the interactive effect of K^+ and Cl^- on force development in mouse skeletal muscle at 37°C, over a wide range of stimulation frequencies. Secondly, experiments were undertaken to determine if a reduction in G_{Cl} could protect against the severe K^+ sensitivity in HEPP. The results show that in wildtype muscle, a reduction in G_{Cl} improved force generation at high $[K^+]_e$ at stimulation frequencies that naturally occur in vivo for mouse EDL and soleus. While the effect in wildtype muscles was proof of principle that a reduction in G_{Cl} may be a potential approach to treat HEPP patients, the effects of reduced G_{Cl} at high $[K^+]_e$ was quite variable in HEPP muscles. In a few cases, lowering G_{Cl} did improve force generation at high $[K^+]_e$. However, in most cases the decrease in G_{Cl} exacerbated the force depression at high $[K^+]_e$, suggesting that more studies will be necessary to understand the variability in the Cl^- effect to conclude whether a decrease in G_{Cl} is a viable approach to treat HEPP patients.

TABLE OF CONTENTS

LIST OF FIGURES

LIST OF ABBREVIATIONS

$[\ ]_i$	intracellular concentration
$[\ ]_e$	extracellular concentration
9-AC	anthracene-9-carboxylic acid
ANOVA	analysis of variance
AP	action potential
ClC-1	chloride channel
DHPR	dihydropyridine receptor
EDL	extensor digitorum longus
E_M	membrane potential
E_{ion}	equilibrium potential for an ion
G_{Cl}	chloride conductance
G_K	potassium conductance
G_{Na}	sodium conductance
HEPP	Hyperkalemic periodic paralysis
HypoPP	Hypokalemic periodic paralysis
Hz	Hertz (frequency)
K_{ATP}	ATP-sensitive K^+ channel
K_{ir}	Inwardly-rectifying K^+ channel
K_V	voltage-sensitive K^+ channel
L.S.D.	least significance difference
MC	Myotonia congenita
mV	millivolt

Na_V	voltage-gated Na^+ channel
N/cm^2	Newton per centimeter square
NKA	Na^+-K^+ ATPase pump
NKCC1	Na^+ K^+ $2Cl^-$ Transporter isoform 1
PKA	protein kinase A
PAM	Potassium-aggravated myotonia
PC	Paramyotonia congenita
S.E.	standard error
SR	sarcoplasmic reticulum

ACKNOWLEDGEMENTS

Firstly, I would like to thank my supervisor, Jean-Marc, for all his help and being patient with me as I broke transducers (more than one!) and as I cried over the stupidity of Microsoft Word during the writing of this thesis! I also appreciate all the encouragement and help from my fellow lab mates: Tarek, Erik, Hind and Wei, as well as everyone else who worked in the lab.

I would also like to thank my advisory committee, Dr. Staines and Dr. Bergeron for their time, advice and excellent questions.

Last but not least, I owe a big thanks to my family, my wonderful sister Melissa, and friends for their support. To Sophie, Tim, Danielle, and Alexis: I could not have gotten through the last 5 months of my Master's if it was not for you. I am forever grateful.

In dedication to my wonderful and beautiful Mother, you always believed in me and I made it this far because of your love and support. You've always been there and I know you will be there in spirit for the rest of life's milestones.

INTRODUCTION

A muscle contraction is initiated when an action potential is generated on the cell membrane. Action potentials are rapid and transient changes in membrane potential (E_M) consisting of two phases: 1) a depolarization phase as the membrane depolarizes from -80 to +30 mV and 2) a repolarization phase as the membrane returns to -80 mV (Ji *et al.*, 1994). They are first generated at the neuromuscular junction where the motor neuron releases acetylcholine. Acetylcholine binds to its ligand-gated nicotinic acetylcholine receptor which opens the receptor's channel. Na^+ influx and K^+ efflux occurs through the channel of the receptors and because the drive for Na^+ influx is greater than that for K^+ efflux, a local depolarization occurs. This depolarization activates the voltage-gated Na^+ channels (Na_V channels) required for the depolarization phase of the action potential.

Once initiated, action potentials spread along the surface membrane (sarcolemma) and propagate down into invaginations of the cell membrane known as transverse tubules (T-tubules). L-type Ca^{2+} channels ($Ca_V1.1$ channels) located along the T-tubular membrane act as voltage sensors and undergo conformational changes in structure upon depolarization. Due to a protein-protein interaction, the $Ca_V1.1$ channel directly activates the ryanodine receptor (Ca^{2+} release channel) located in the sarcoplasmic reticulum (SR), which are the Ca^{2+} stores in muscle (Dirksen & Beam, 1999). The released Ca^{2+} then diffuses to the sarcomeres within the muscle to initiate contraction. Sarcomeres are the functional unit of contractility meaning they contain all the structures required for muscle shortening and contraction. They contain the two contractile proteins: 1) myosin, on the thick and 2) actin on the thin filament. Sarcomeres

also contain two regulatory proteins located on the thin filaments, troponin and tropomyosin, that interact with Ca^{2+} to start contraction. At rest, the myosin binding site on action is blocked by tropomyosin. As Ca^{2+} binds to troponin C, the subsequent conformational change in troponin T moves tropomyosin away from the myosin binding site on actin (Gordon *et al.*, 2000). When myosin binds to actin, energy in the form of ATP is used to change the shape of the myosin protein. This pulls the thin filament towards the center of the sarcomere, causing shortening and contraction. Once stimulation ceases, Ca^{2+} is sequestered back into the SR by Ca^{2+}-ATPase pumps, allowing for the muscle to relax.

The capability of muscles to generate normal action potentials depends on the maintenance of the surface membrane's excitability. Impairment of membrane excitability can lead to either enhanced excitability (hyperexcitability) or depressed excitability (hypoexcitability). Hyperexcitability occurs when excitatory ion channels (e.g., Na_V channels) frequently open in the absence of neural stimulation, resulting in myotonic discharges, which are repetitive and uncontrolled contractions. Conversely, hypoexcitability occurs when excitatory channels are incapable of opening upon stimulation, resulting in paralysis. These impairments are common in diseases referred to as channelopathies and are caused by mutations in ion channels of skeletal muscle. One of these channelopathies is hyperkalemic periodic paralysis (HEPP). HEPP is caused by mutations in the gene that encodes for the voltage-gated Na^+ channel (Na_V), causing them to frequently open at rest (Cummins *et al.*, 1993). Myotonia occurs first as the resting membrane potential moves toward the threshold for action potential generation, causing action potentials to fire uncontrollably. As myotonia persists, an accumulation of

extracellular K^+ ($[K^+]_e$) occurs. High $[K^+]_e$ further destabilizes the membrane potential, eventually leading to paralysis as Na_V channels become unresponsive to stimulation. The paralysis is temporary and is alleviated once the accumulated K^+ is removed or redistributed across the sarcolemma.

Current treatments are often ineffective or become ineffective over time (Miller *et al.*, 2004;Clausen *et al.*, 2004). Therefore, there is a need for new pharmacological strategies for the treatment of HEPP patients. It is now known that reducing Cl^- channel activity alleviates K^+-induced force depression in normal, healthy muscle by improving action potential generation (Pedersen *et al.*, 2005). Therefore, the overall objective of this study was to document whether reduction in Cl^- channel activity can effectively alleviate K^+ sensitivity and prevent paralysis in HEPP muscles.

MEMBRANE POTENTIAL

The cell membrane potential (E_M) is an electrical potential created by unequal amounts of positive and negative charges across the sarcolemma. During rest, the membrane potential lies at a negative value of -80 mV (Yensen *et al.*, 2002). E_M is primarily influenced by the movement of Na^+, Ca^{2+}, K^+ and Cl^- across the sarcolemma. The direction and magnitude of ion movement across the membrane is a function of concentration and electrical gradients, as well as their cell membrane permeability. K^+, for example, has an extracellular concentration of 4-5 mM compared to 140-180 mM in the intracellular space (Green *et al.*, 1999;Green *et al.*, 2000;Juel *et al.*, 2000;Nielsen *et al.*, 2004;Street *et al.*, 2005). As K^+ moves outward and down its concentration gradient, the amount of positive charge within the muscle is reduced making E_M more negative. K^+, however, is also driven inward down the electrical gradient and when the two

opposing fluxes become equal in magnitude, then K^+ is at equilibrium. The membrane potential at which K^+ is at equilibrium is the electrochemical equilibrium, or E_K. At rest, E_M lies at -80 mV, but E_K is -90 mV. Consequently, there is a constant K^+ efflux at rest, which tends to hyperpolarize the cell membrane (Begenisich & Cahalan, 1980). However, E_M never reaches E_K because of the influence from other ions. Cl^- has a depolarizing effect when resting E_M is more negative than -66 mV because it drives resting E_M towards E_{Cl} of -66 mV, however as resting E_M becomes less negative than -66 mV, Cl^- has a hyperpolarizing influence driving E_M back to -66 mV . For Na^+, E_{Na} is +60 mV and therefore its influx also depolarizes the membrane (Begenisich & Cahalan, 1980). Consequently, Cl^- is referred to as a shunt or inhibitory current because it opposes the depolarizing effect by Na^+.

The driving force for the efflux of K^+ and Cl^- and the influx of Na^+ is directly related to the difference between the ion's equilibrium potential and E_M, which would imply that Na^+, with the greatest driving force, would have the largest influence on resting E_M. However, E_M also depends on ion permeability (P_{ion}), which is determined by the activity of their specific ion channel. At rest, Na_V and Ca_V channels are closed, while ClC-1 Cl^-, K_{ATP} and Kir2.1 K^+ channels are open. In skeletal muscle fibers, the ion permeability at rest (P_K:P_{Na}:P_{Cl}) is 1:0.01:10. Therefore Cl^- and K^+ both largely control resting E_M, while Na^+ has minimal influence (Brown & Adams, 1980;Pedersen *et al.*, 2009b). While Na^+ is referred to as excitatory, Cl^- and K^+ are both inhibitory as they maintain the negative resting E_M as well as aiding in the termination of action potentials.

Na_V channels are also referred to as voltage-gated because they open upon a depolarization at a threshold of -40 mV. When this E_M is reached the open probability of

Na_V channels increases, enhancing Na^+ permeability several fold that largely exceeds K^+ and Cl^- permeability. As a consequence of a large permeability and driving force, Na^+ becomes the dominant ion affecting E_M, allowing for the rapid action potential depolarization phase that shifts E_M from -80 mV towards E_{Na}. However, E_M never reaches E_{Na} for three reasons: 1) Na_V channels inactivate within a msec; 2) K_V channels open and repolarize the membrane; 3) ClC-1 Cl^- channels also contribute to the membrane repolarization when E_M is less negative than E_{Cl}.

When several action potentials are rapidly generated, an accumulation of intracellular Na^+ and extracellular K^+ occurs, causing a decrease in their normal resting concentration gradients. This can further depress generation of normal action potentials as the driving force for Na^+ influx and K^+ efflux is reduced. Na^+-K^+ ATPase (NKA) pumps have an important role in restoring these normal gradients to ensure that membrane excitability is maintained by pumping 3 Na^+ out for every 2 K^+ moved into the muscle fiber (Clausen *et al.*, 1998). The pump is therefore also electrogenic, hyperpolarizing resting E_M.

In summary, E_M is a function of ion fluxes across the cell membrane and in turn ion fluxes are regulated by the activities of several ion channels and NKA pumps. Therefore, any perturbation in the normal activity of an ion channel has profound effects on E_M and ultimately on membrane excitability and contractility. This is the basis for channelopathies, which are disorders caused by mutations in the genes encoding for ion channels.

CHANNELOPATHIES

Channelopathies in skeletal muscle comprise a wide spectrum of symptoms

emanating from changes in membrane excitability. At one end of the spectrum, excitability is abnormally increased and at the other end of the spectrum, excitability is completely lost. Hyperexcitable muscles exhibit bursts of action potentials long after neural stimulation has ceased, causing myotonia (Fig. 1-1). Patients perceive this as severe muscle stiffness. Two disorders exhibit purely myotonia and include Myotonia congenita (MC) and Paramyotonia congenita (PC). Dominant MC (Thomsen's disease) is caused by mutations or premature stops near the carboxyl terminus of the ClC-1 Cl^- channel. Recessive MC (Becker's disease) is caused by deletions, insertions, or missense mutations in the same channel (Pusch, 2002;Cannon, 2006). These mutations result in 80% or greater reductions in Cl^- conductance (Adrian & Bryant, 1974). Potassium-aggravated myotonia (PAM) is due to missense mutations encoding the skeletal muscle specific voltage-gated Na^+ channel. Cl^- conductance is normal in PAM however, upon a "potassium challenge" where plasma or interstitial K^+ is increased PAM muscles exhibit a large persistent Na^+ current and subsequent myotonia (Lehmann-Horn *et al.*, 1983). Hypoexcitable muscles exhibit profound weakness leading to episodic paralysis that can last from minutes to days. A square electrical pulse stimulation provokes an action potential in normal muscle (Fig. 1-1). However, for a paralyzed muscle for which the membrane is largely depolarized, the same stimulation fails to generate an action potential. Between sets of paralytic attacks, muscle function is often normal, but a constant and progressive myopathy usually develops overtime. Paralysis occurs in both Andersen-Tawil syndrome and hypokalemic periodic paralysis (HypoPP). Andersen-Tawil syndrome is caused by missense mutations or in-frame deletions in the gene encoding for the inwardly-rectifying K^+ channel (Kir2.1) (Plaster *et al.*, 2001).

FIGURE 1-1

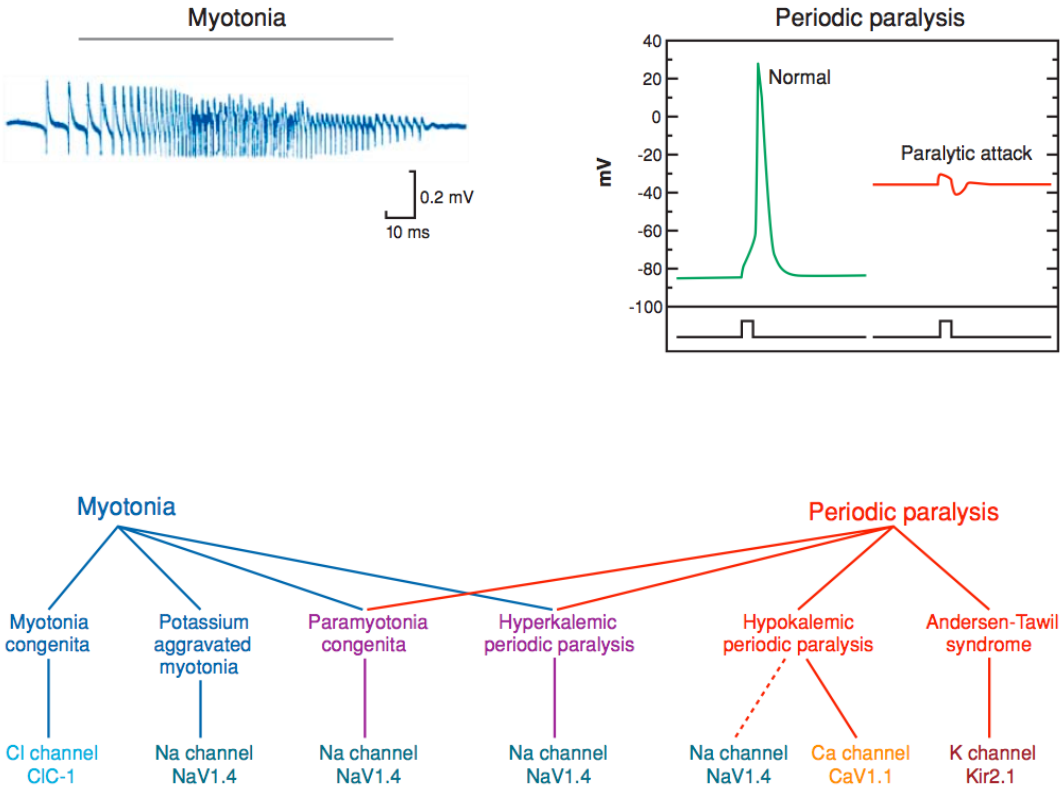

Figure 1-1. Channelopathies of skeletal muscle cause impairments in excitability and a wide spectrum of symptoms from myotonia to periodic paralysis. *Top left:* Electromyography recording of myotonic bursts. *Top right:* Computer simulation of a square pulse stimulus-induced generation of an action potential in normal muscle and failure in paralyzed muscle. *Bottom:* Clinical spectrum of channelopathies afflicted by myotonia or periodic paralysis. The nature of the voltage-gated ion channel causing the defect is listed underneath. Disorders exhibiting both myotonia and paralysis are all caused by mutations in the $Na_V1.4$ Na^+ channels (Fig. from Cannon, 2006).

HypoPP is caused by missense mutations either in the gene encoding for the voltage-sensitive Ca^{2+} channel $Ca_V1.1$, or in $Na_V1.4$ and results in reduced ionic current and slowed activation (Fontaine *et al.*, 1994). In both disorders, a reduction in $[K^+]_e$ triggers paralysis (Matthews *et al.*, 2010).

Two channelopathies identified so far show symptoms of both myotonia and paralysis: Paramyotonia congenita (PC) and Hyperkalemic periodic paralysis (HEPP) (Fig. 1C). These disorders are caused by missense mutations in the gene encoding for the skeletal muscle Na_V channel (Cannon, 2002;Lehmann-Horn, 2004). Paralytic attacks in HEPP are triggered at high plasma K^+ levels. It is important to note that while PAM, PC, HEPP and HypoPP are all due to mutations of the Na_V channel, the difference in symptoms depend on the location of the mutation in the protein and its effect on the channel's electrophysiological properties (see section "Voltage-gated Sodium Channels" for further details).

HYPERKALEMIC PERIODIC PARALYSIS

Hyperkalemic periodic paralysis (HEPP) is a dominant disorder with almost complete penetrance (>90%), affecting around 1 in 200,000 people (Jurkat-Rott & Lehmann-Horn, 2007b). Myotonia is seen in 70% of patients and sometimes patients remain asymptomatic. Paralysis mainly affects the lower limbs and can leave patients debilitated and bed-ridden during the attack. Common triggers include high-potassium foods, rest after exercise, cold exposure and emotional stress. Due to a marked sensitivity to K^+, the ingestion of KCl is often used as a provocative test by doctors to diagnose patients with the disorder (Miller *et al.*, 2004). While it does not affect normal

individuals, the rise in K^+ triggers a paralytic attack 100% of the time in HEPP patients (see section "Molecular to Physiological Defect" for further explanation).

Nine different missense mutations in the Na_V 1.4 channel can cause HEPP. The two most common mutations are the replacement of threonine by methionine at position 704 (T704M) and the replacement of methionine by valine at position 1592 (M1592V). The frequency and duration of paralytic attacks are highly variable between patients and often depends on the mutation (Table 1-1). Patients with the T704M mutation have on average one attack per day and those with M1592V only three attacks per month. However, attacks are much shorter for T704M patients, being on average 8 hours, compared to 89 hours for M1592V patients (Miller *et al.*, 2004). Patients with the T704M mutation often experience their first paralytic attack at around 8 months old, whereas patients with the M1592V mutation often do not experience their first attack until five years of age (Miller *et al.*, 2004; (Jurkat-Rott & Lehmann-Horn, 2007b). For all HEPP cases, the frequency and severity of the attacks increase during adolescence and early adulthood. After the age of 30, attacks usually become less prominent and are replaced with a progressive and permanent weakness causing myopathy (Jurkat-Rott & Lehmann-Horn, 2007b). This makes walking difficult for adults with HEPP and causes some patients to be wheel-chair bound (Pearson, 1964) To better understand how mutations in the $Na_v1.4$ channel cause myotonia and paralysis, the structure and function of normal Na_V channels will first be thoroughly discussed.

VOLTAGE-GATED SODIUM CHANNELS

Voltage-gated Na^+ channels are mainly found in excitable tissues where they generate action potentials in pancreatic α-cells, neurons, cardiac and skeletal muscle

TABLE 1-1

Summary findings	HyperKPP with mutations: Sodium channel (*SCN4A*) T704M mutation (n = 50)	HyperKPP with mutations: Sodium channel (*SCN4A*) M1592V (n = 13)	All HyperKPP mutations (n = 82)	HyperKPP without mutations (n = 17)
Age at onset, y	0.8 ± 0.8	5 ± 4	2 ± 4	14 ± 14
Average ± SD	0–0.9	0–10	0–16	5–61
	(n = 39)	(n = 13)	(n = 63)	(n = 16)
Frequency of attacks/mo				
Average ± SD	28 ± 12	3 ± 2	16 ± −16	6 ± 6
Range	8–42	5–6	1–42	1–16
	(n = 17)	(n = 4)	(n = 26)	(n = 4)
Duration, h				
Average ± SD	8 ± 28	89 ± 58	24 ± 42	23 ± 18
Range	0.3–168	24–144	2–72	2–48
	(n = 41)	(n = 7)	(n = 56)	(n = 8)
Usual precipitants, %				
Exercise	83	73	80	69
Cold	58	38	54	38
Hunger	29	13	25	6
Stress	46	13	34	19
Illness	0	38	30	
Potassium rich foods	32		21	
Other	25	38	8	13
	(n = 41)	(n = 11)	(n = 64)	(n = 16)

Table 1-1. Clinical data for Hyperkalemic Periodic Paralysis. Patients with the $Na_V1.4$ (SCN4A) T704M mutation experience onset of symptoms at an earlier age compared to patients with the M1592V mutation. T704M patients also have more frequent and severe attacks of weakness, although the attacks are much shorter in duration than in M1592V patients. (Table from Miller *et al.*, 2004).

fibers. To date, nine genes have been identified encoding for $Na_V1.1$ to 1.9 (Ashcroft. 2000). $Na_V1.1$-1.3 and 1.8 are found within the central and peripheral nervous system; Na_V 1.5 is expressed in cardiac and embryonic skeletal muscle; while $Na_V1.4$ is expressed in adult skeletal muscle. $Na_V1.4$ is encoded by the SCN4A gene and is located on chromosome 17q23-q25 (Ebers *et al.*, 1991).

Structure

Like all voltage-sensitive cation channels (Na_V, K_V, Ca_V), Na_V channels are composed of two subunits, α and β, being in a 1:1 ratio for $Na_V1.4$. When expressed in oocytes, the α subunit expresses a completely functional channel, but exhibits slower current termination. The β-subunit is composed of a single transmembrane segment with a glycosylated extracellular domain and is believed to stabilize the α-subunit gating as it enhances the Na^+ current and increases the rate of inactivation (refer to section on inactivation below) (Isom *et al.*, 1994;Ji *et al.*, 1994).

The α subunit consists of ~2000 amino acids divided into four homologous repeats or domains (DI-DIV) that assemble into a complex with a central permeation pore. Each repeat includes six transmembrane α-helix segments (S1-S6) (Fig. 1-2). Segments S1 to S3 surround the structure and interact with the membrane lipid bilayer. S4 segments are completely surrounded by the other membrane spans and are placed centrally within each domain. S4 segments act as the channel's voltage sensors. The region between S1 and S2, referred to as SS1-SS2, contains a ring of negatively charged glutamates or aspartic acids (EEDD). The first two SS1-SS2 regions (i.e. on DI and DII) contain glutamate (E), while the other two SS1-SS2 regions (i.e. on DIII and DIV) contain aspartic acid (D). These negatively charged residues attract cations (Na^+, K^+, Ca^{2+}) and repel anions (Cl^-). The S5 and S6 segments line the channel pore while the

FIGURE 1-2

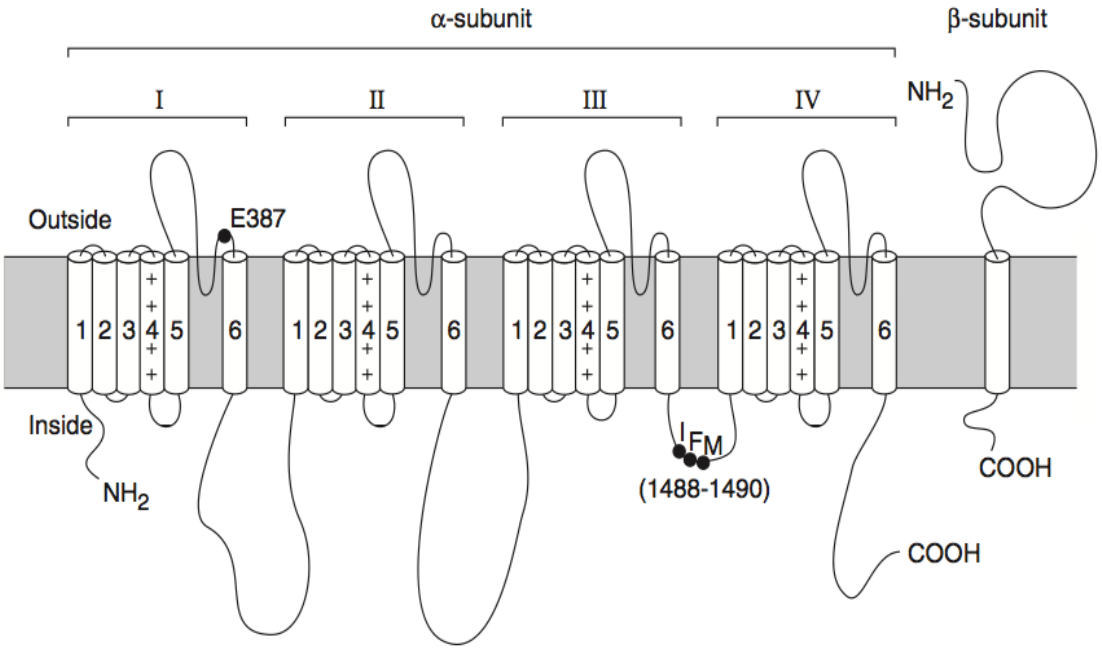

Figure 1-2. Putative structure for the skeletal muscle voltage-gated Na^+ channel, NaV1.4. Note the 1) positively charged residues in S4 that make up the voltage sensor; 2) extracellular P-loops between transmembrane spans 5 and 6 of each domain line the pore and contribute to the selectivity filter; and 3) the intracellular loop between III and IV with the IFM "particle" associated with fast-inactivation (Fig. from Ashcroft, 2000).

connecting linkers (P-loops) dip into the channel's pore to create the selectivity filter (Fig. 1-2).

The P-loops are responsible for the ion selectivity and contain a conserved sequence of amino acids located deep within the pore. For Na^+ selectivity, each P-loop contains a single critical amino acid which includes: a negatively charged aspartic acid (D) in DI; a negatively charged glutamate residue (E) in DII; a positively charged lysine (K) in DIII; and a neutral alanine (A) in DIV. Substituting all four residues (DEKA) with negatively charged glutamate residues (EEEE) causes Na^+ channels to lose their selectivity for Na^+ and gain selectivity for Ca^{2+} (Terlau *et al.*, 1991). The ring of charged residues in the Na_V channel also discriminate Na^+ from K^+, as the channel is 10-fold more permeable to Na^+. The two ions are discerned from one another by their differences in size, as the radius of the dehydrated Na^+ is 0.95 Å and that of K^+ is 1.33 Å (Sun *et al.*, 1997;Ng *et al.*, 2008). Hence, the size of the pore in the Na_V channel is large enough to permit passage to Na^+, but not K^+.

Activation

Activation of Na^+ channels is important for initiating the depolarization phase of the action potential. A depolarization to -40 mV from a holding potential of -100 mV is required for activation, with half the channels ($V_{1/2}$) activated by -16 mV and full channel activation by +20 mV (Cummins *et al.*, 1993) (Fig. 1-3). As mentioned above, the voltage sensing mechanism primarily lies within the S4 segment of each domain. The S4 segments have an α-helix structure with positively charged amino acids, either lysine or arginine, at every third position. Substitution of a single positively charged residue with a neutral residue weakens the voltage sensitivity of the channel by shifting the voltage of activation to more positive values. For example, by mutating the lysine in the S4 of

FIGURE 1-3

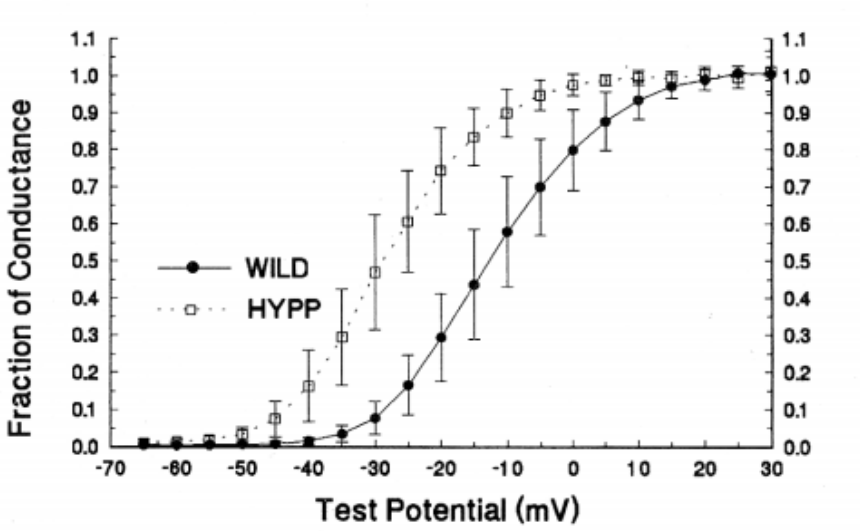

Figure 1-3. Steady-state voltage-dependent activation of wildtype and HEPP Na^+ currents. Measurements were recorded from HEK cells containing either the normal $Na_V1.4$ channels or the rat homologue mutation, T698M. Holding potential was -100 mV. The voltage dependent activation of the HEPP channels is shifted 15 mV in the hyperpolarizing direction (Fig. from (Cummins *et al.*, 1993).

domain I to glutamine (1K4Q) there is a shift in activation, $V_{1/2}$ and full activation to -35 mV from -40 mV, -10 from -16 from and 10 mV from +20 mV, respectively (Kontis *et al.*, 1997). It has been proposed that upon depolarization, the positively charged residues in S4 segments move outwards toward the extracellular membrane surface and that by an unknown mechanism it opens the pore (Noda *et al.*, 1984).

Deactivation & Inactivation

At rest the activation gate, composed of the S4 segments, is closed. In this state, $Na_V1.4$ channels are deactivated and Na^+ is prevented from moving through the pore. The activation gate rapidly opens upon depolarization and only closes upon repolarization. The issue that arises is how exactly the $Na_V1.4$ channels close at the peak of the action potential to allow for action potential termination; i.e. repolarization. A second mechanism is thus necessary. This involves an inactivation process, which closes the channel's pore during prolonged depolarization and makes the channels voltage-unresponsive until the membrane has been repolarized. For $Na_V1.4$, there are two structurally and kinetically different gating components for inactivation, known as fast and slow inactivation.

Fast Inactivation

Fast inactivation occurs at the peak of the action potential and is responsible for: 1) termination of the depolarization phase of the action potential and 2) assures unidirectional propagation of action potentials as it renders the channels incapable of re-opening until the membrane potential returns back to -80 mV.

The gating mechanism involves a portion of the protein on the cytoplasmic side which was found by internally perfusing pronase, a proteolytic enzyme that cleaves

peptides, resulting in the removal of inactivation but not activation (Bezanilla & Armstrong, 1977) It is now known that each Na^+ channel has a single inactivation particle located on the cytoplasmic loop connecting DIII to IV, which contains an IFM motif ("the lid"), composed of three amino acids isoleucine (I), phenylalanine (F) and methylalanine (M) (Fig. 1-2). The IFM motif is linked to glycine and proline residues that act as a "hinge" (Amin *et al.*, 2010). Fast inactivation is initiated as the S4 segments moves outward from the membrane in response to depolarization. This triggers the IMF motif and hinge to move and block the inner vestibule of the channel pore by interacting with other amino acids located between S4 and S5 segments of DIII and DIV ("the dock") (Amin *et al.*, 2010).

Steady-state measurements show that fast inactivation begins at -60 mV, with 50% of the channels inactivated at -30 mV and complete inactivation at -10 mV (Fig. 1-4). Compared to the voltage-dependence of activation (shown above), fast-inactivation occurs at more negative potentials. However, because fast-inactivation is slower, activation occurs before the channels inactivate. For example, with a depolarization to +30 mV, the time constant for inactivation (τ_h) is 0.67 msec compared to only 0.14 msec for activation (τ_m) (Hodgkin & Huxley, 1952). This delay allows ample time for Na^+ influx during the rise of the action potential before channels become inactivated (Armstrong & Hille, 1998). As the membrane repolarizes back to -80 mV, all four S4 segments move back to their resting positions, causing the inactivation particle to detach from the pore. The time constant for recovery is about 15 msec (Bendahhou *et al.*, 1999).

Potassium aggravated myotonia (PAM) and Paramyotonia congenita (PMC) are two channelopathies caused by mutations of the $Na_V1.4$ Na^+ channel. The mutations

FIGURE 1-4

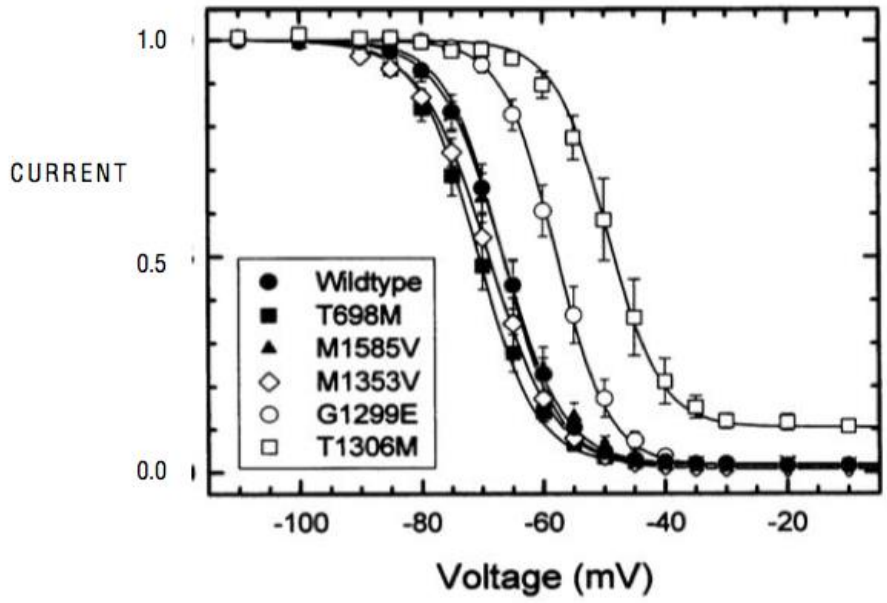

Figure 1-4. Voltage-dependence of fast-inactivation in wildtype and mutant Na_V channels. Peak Na^+ current was measured upon depolarization to -10 mV after a conditioning pulse of 5 msec from -140 to -10 mV. T698M and M1585V are the rat homologues for the two most common HEPP mutations while M1353V is a third variant of HEPP. G1299E is a mutation in Potassium aggravated myotonia (PAM) and T1306M in Paramyotonia congenita (PMC). Defects in fast-inactivation occur for the SCM and PMC mutants. A relative current of 1 means that none of the channels were fast-inactivated, while the reverse is true for a relative current of 0 (Fig. from Hayward *et al.*, 1997).

cause impairments in fast-inactivation, as the voltage-dependence is shifted rightward, to more depolarized potentials (Fig. 1-4). The mutant channels also exhibit a three- to five-fold slowing in fast-inactivation (Cannon, 2006) (Yang et al., 1994). The slowing of fast-inactivation prolongs the duration of action potentials and increases the amount of Na^+ channels still available at the end of each action potential, causing hyperexcitability and myotonia.

Slow Inactivation

Na^+ channels can enter into a second type of inactivated state, known as slow inactivation, in the presence of prolonged depolarization. Slow-inactivation is kinetically distinct from fast-inactivation as its initiation and recovery requires several seconds to minutes long to occur. For example, slow-inactivation took ~13 seconds to be initiated after a 5 second depolarization to -20 mV and took 40 seconds to be released from that inactivated state (Cummins & Sigworth, 1996). Hence, slow inactivation is too slow to regulate individual action potentials that occur within 1-2 msec. Rather, it regulates the overall availability of Na_V channels over time and decreases its availability during these prolonged depolarizations. The voltage-dependence for slow-inactivation was examined after a 50 second depolarization (Fig. 1-5). At rest, for which E_M is -80 mV, one third of the channels were slow-inactivated; 50% were slow-inactivated at -60 mV and all were fully inactivated by -10 mV.

Slow-inactivation is structurally distinct from fast-inactivation as it remains intact even after internally perfusing with pronase or mutating the IFM motif to QQQ (glutamine) (Cummins & Sigworth, 1996;Featherstone *et al.*, 1996). The gating mechanism has yet to be fully elucidated, however it is believed that the gates are located within the P-loops between segments S5 and S6 where they interact to line the pore

FIGURE 1-5

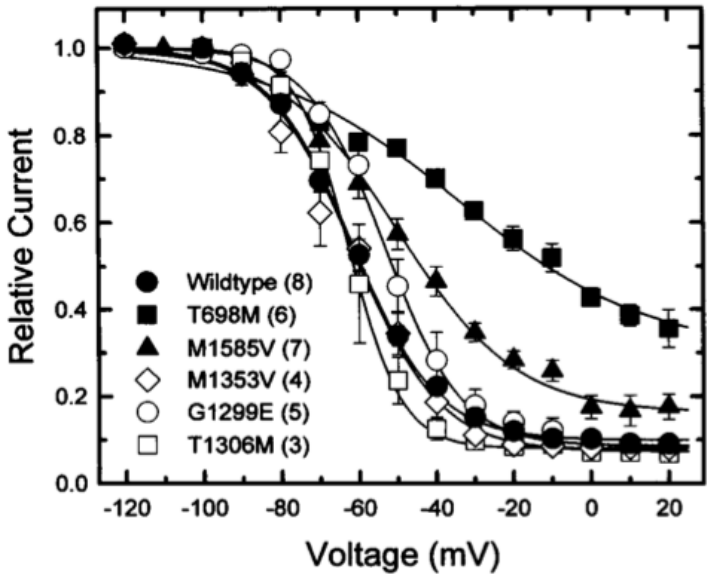

Figure 1-5. Steady-state voltage-dependence of slow-inactivation for wildtype and mutant $Na_V1.4$ channels. From a holding potential of -100 mV, a 60 sec conditioning pulse to potentials between -120 and +20 mV were tested. Fast inactivation was then removed with a 20 msec pulse to -100 mV before the remaining Na^+ current was measured at -10 mV. T698M and M1585V are the rat homologues for the two most common HEPP mutations while M1353V is a third variant of HEPP. G1299E is a mutation in Potassium aggravated myotonia (PAM) and T1306M in Paramyotonia congenita (PMC). A relative current of 1 means none of the channels were slow inactivated, while the reverse is true for a relative current of 0. (Fig. from Hayward *et al.*, 1997).

(Zhou *et al.*, 2001). This was made evident by mutating the DEKA residues in the selectivity filter which actually promoted channel slow-inactivation (Hilber *et al.*, 2005). In addition, mutations in the EEDD ring located in the outer portion of the pore also affected slow-inactivation (Zhang *et al.*, 2003). It is hypothesized that slow-inactivation also depends on the ionic environment as findings show that Na^+ has a neutralizing and stabilizing effect in the outer pore of the channel. In the absence of Na^+, the carboxylates (COO^-) in the EEDD residues are repulsed from one another, causing the ring to rearrange and form a non-conducting pore (Tikhonov & Zhorov, 2007).

Impairments in slow-inactivation have been identified in four channelopathy mutations to date, of which all are associated with paralytic phenotypes as seen in hyperkalemic periodic paralysis (HEPP) and PMC (Fig. 1-5). As mentioned above, the two most common mutations in HEPP are T704M and M1592V. T704M is located on segment S5 of DII, while M1592V is on S6 of DIV of the Na^+ channel. It is not known exactly how the mutations in these locations give rise to HEPP symptoms, however it is known that three distinct defects arise in the channel from these mutations (Jurkat-Rott & Lehmann-Horn, 2006).

MOLECULAR MECHANISMS OF HEPP MUTATIONS

The first defect in HEPP Na^+ channel activity is a hyperpolarizing shift in the voltage-dependent activation curve, causing enhanced activation (Fig. 1-3). As a result, mutant channel activation begins at a more negative potential than normal: by -60 mV as opposed to -40 mV in normal $Na_V1.4$ channels; with a $V_{1/2}$ of -28 mV compared to -16 mV; and full activation by -10 mV compared to +20 mV. This also means that for a given potential between -60 mV and 20 mV, there is a larger Na^+ current in HEPP mutant

channels. For example, by -30 mV there is a 5-fold larger Na^+ current in HEPP compared to wildtype (Cummins et al. 1994). While fast inactivation is not affected (Fig. 1-4), the second defect is a shift in the steady-state slow-inactivation curve to less negative potentials (Fig.1-5). For example, the $V_{1/2}$ for channel slow-inactivation in the HEPP T696M (rat homologue) channel was shifted from -60 mV (wildtype) to -10 mV, while for the M1585V mutation it was shifted to -30 mV. Even by +20 mV when normal Na^+ channels were all inactivated, a non-inactivating current of about 20-30% of control was observed in the mutated Na^+ channels (Hayward *et al.*, 2007).

Unlike wildtype Na^+ channels, HEPP mutant channels are directly altered by high extracellular K^+, ($[K^+]_e$), contributing to the third defect. To examine the K^+ effect, single-channel recordings were conducted on myotubes developed by incubating satellite cells from human muscle biopsies of normal and HEPP patients. At normal 3.5 mM K^+, a depolarizing step from -70 to -30 mV activated an inward Na^+ current that inactivated within 2 msec in both normal and HEPP myotubes (Fig. 1-6A and B). At 10 mM K^+, normal openings and inactivation were observed for normal Na^+ channels (Fig. 1-6C), but caused 10-15% of HEPP Na^+ channels to enter a non-inactivating mode, as they persistently opened throughout the 15 msec depolarizing step (Fig. 1-6D). As the membrane potential was maintained at -30 mV by voltage-clamping, the loss of inactivation was not due to a K^+-induced depolarization effect. Rather, it was suggested that K^+ directly affected the gating of the HEPP channels, triggering the non-inactivating current.

MOLECULAR TO PHYSIOLOGICAL DEFECT

As mentioned above, one-third of normal Na^+ channels are slow-inactivated at

FIGURE 1-6

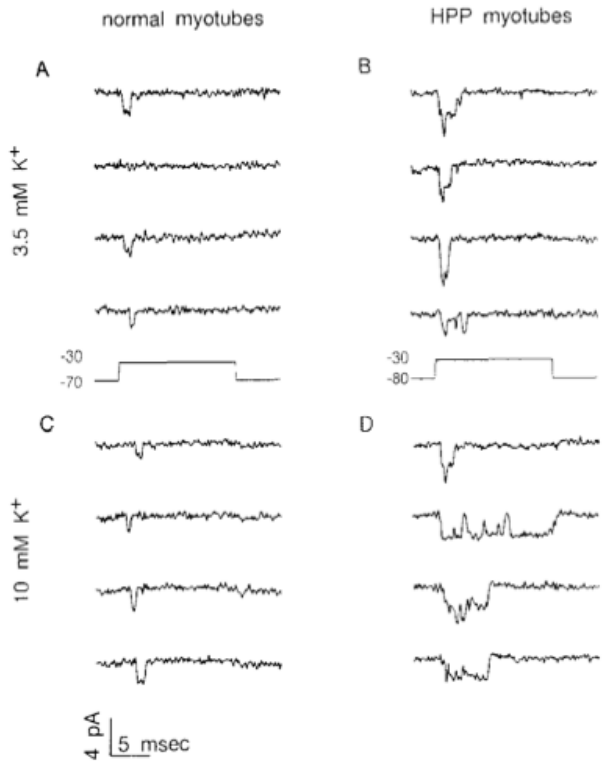

Figure 1-6. Single Na^+ channel gating in normal and HEPP myotubes. The membrane was voltage-clamped and Na^+ currents were measured during 15-msec depolarizing steps. In normal myotubes, the inward current was of short duration because of rapid inactivation, at both 3.5 and 10 mM K^+. For HEPP channels, the inward Na^+ current was normal at 3.5 mM K^+, while at 10 mM K^+, prolonged Na^+ currents were observed throughout the 15 msec depolarization step as mutant channels entered a non-inactivating mode (Fig. from Cannon *et al.*, 1991).

rest. Due to the impairment in slow-inactivation in HEPP: less channels are inactivated at rest, causing a larger than normal Na^+ influx (700 compared to 400-500 nmoles/g wet weight/min in wildtype) and a depolarization of resting E_M towards -60 mV (Lucas *et al.*, 2014;Clausen *et al.*, 2011). Furthermore because of the large shift in the activation curve, Na^+ channels open more easily at negative potentials near resting E_M (Fig. 1-7). Another consequence of the defect is a lower than normal action potential threshold. Overall, with a smaller resting E_M and threshold in HEPP, this increases the probability of generating action potentials in the absence of stimulation from the motor neuron (i.e. myotonia). Persistent myotonic discharge eventually leads to an accumulation of extracellular K^+, which has two effects: 1) further increases Na^+ influx by triggering the non-inactivating mode of mutant Na^+ channel, and 2) causes large depolarizations, as an increase in $[K^+]_e$ from 4.7 to 7 mM causes a 30 mV depolarization in HEPP compared to 10 mV in wildtype (Cannon *et al.*, 1991). The large depolarization eventually leads to the inactivation of all normal $Na_V1.4$ channels and enough of the mutant ones to cause a complete loss of membrane excitability and thus paralysis. The paralysis persists until the depolarization is removed and the time course of recovery from slow-inactivation has lapsed.

TREATMENTS FOR HYPERKALEMIC PERIODIC PARALYSIS

HEPP symptoms cannot simply be prevented by using a Na^+ channel blocker such as tetrodotoxin (TTX) as it is not specific to skeletal muscle. Cardiac isoforms Na_V 1.5, 1.8 and 1.9 are slightly less TTX sensitive (IC_{50} ~1 μM), while skeletal and nervous system isoforms are highly sensitive (IC_{50} ~10 nM) (Zimmer, 2010). In animal models, sub-lethal doses of TTX impaired neurological and neuromuscular functions, all of which

FIGURE 1-7

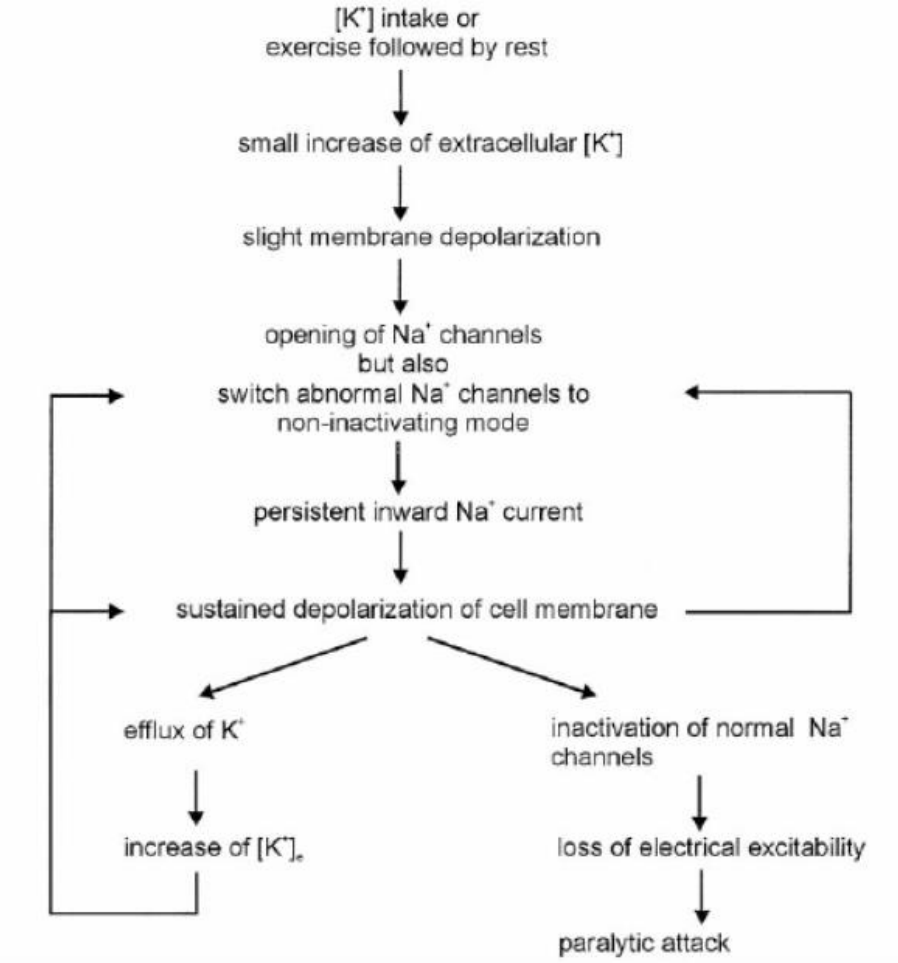

Figure 1-7. Putative pathomechanism in mutant HEPP Na^+ channels leading to myotonia and paralysis. (Fig. from Lehmann-Horn & Jurkat-Rott, 1999).

are controlled by TTX-sensitive Na^+ channels. Symptoms included vomiting, diarrhea, absence of reflexes, ascending progressive paralysis and respiratory pattern changes. Death ensued due to TTX blockade in the respiratory system, including inhibition of the phrenic nerve, diaphragm and neurons in the central respiratory network (Chang *et al.*, 1990).

Current treatment options for HEPP include: 1) carbonic anhydrase inhibitors; 2) calcium gluconate; 3) ß-adrenergic receptor agonists and 4) thiazide diuretics. Acetazolamide, a carbonic anhydrase inhibitor, is used to prevent secretion and buildup of fluids that occurs in diseases such as glaucoma and edema. For patients suffering of hypo- and hyperkalemic periodic paralyses, it is used as a prophylactic to reduce frequency of attacks, but it does not alleviate severity (Pearson, 1964). The mechanism of action of acetazolamide is unclear, but may involve activation of Ca^{2+}-activated K^+ (K_{Ca}) channels allowing for a hyperpolarization of the cell membrane, reducing the possibility of myotonia (Mallouk & Allard, 2000). Calcium gluconate is commonly used to reduce the severity of attacks; however it is ineffective in reducing the frequency of attacks (Pearson, 1964). Calcium alleviates the severe depolarization as it reduces the excessive Na^+ influx by shifting the voltage-dependence of activation of $Na_V1.4$ channels to more depolarized potentials (Lucas *et al.*, 2014;Campbell & Hahin, 1984). The ß-adrenergic receptor agonist, salbutamol, is beneficial because it provides both a hyperpolarizing and hypokalemic influence important for alleviating weakness. The mechanism of action is through stimulation of the cAMP/PKA signaling pathway that ultimately upregulates Na^+-K^+ ATPase pump activity (Clausen *et al.*, 1998). Thiazide diuretics are also often

used on a continuous basis to stabilize plasma potassium levels (Jurkat-Rott & Lehmann-Horn, 2007a).

Unfortunately, none of these treatments are fully effective or they often become ineffective with time. For example, most patients with the T704M mutation are unresponsive to acetazolamide, while the rest report loss of effectiveness with time (Miller *et al.,* 2004). Additionally, because salbutamol is also used as a bronchodilator in the treatment of asthma, adverse lung function can occur with long-term use. Adverse functions include paradoxical bronchospasms, which means that constriction of the bronchioles occurs rather than the normal dilation response (Wraight *et al.,* 2004). The focus taken in this study then was to find a potential new pharmacological approach to treat HEPP patients. One such approach is a reduction in chloride conductance (G_{Cl}) to reduce the K^+-induced loss of membrane excitability.

ION MODULATION OF MEMBRANE EXCITABILITY & CONTRACTILITY

K^+ EFFECT

During exercise or increased muscular activity, plasma $[K^+]$ increases from a resting level of 4 mM to a venous concentration of 7 mM (Juel *et al.,* 1990;Sejersted & Sjogaard, 2000). The concentration is even greater in the muscle interstitium, as the volume of the space is much smaller. Interstitial K^+ can increase from ~4 to 12 mM, even 14 mM in some individuals, during the first five minutes of moderate muscle activity (Street *et al.*, 2005;Nielsen *et al.*, 2004). The accumulation of K^+ is due to the large efflux through K_V channels when multiple action potentials are rapidly generated and the rate of reuptake by Na^+-K^+ ATPase does not match the rapid efflux. As a consequence of higher $[K^+]_e$, the cell membrane depolarizes. For example, an increase in $[K^+]_e$ to 12 mM can

generate a 25 mV depolarization and causes more than 50% of the voltage-gated Na^+ channels to slow-inactivate (Cairns *et al.*, 1997) (Fig. 1-5). Such large channel inactivation reduces the peak of the action potential from ~30 mV to <10 mV, subsequently decreasing Ca^{2+} release and force (Yensen *et al.*, 2002;Cairns *et al.*, 1997). Exposing muscles to caffeine, which increases Ca^{2+} release from the SR, increases force at high $[K^+]_e$. This suggests that Ca^{2+} release is indeed reduced at high $[K^+]_e$ and therefore explains for the loss of force (Cairns *et al.*, 1997).

The effect of high $[K^+]_e$ on contractile force is dynamic and thus is far more complex than as described above. Several factors modulate how high $[K^+]_e$ affects force (McKenna *et al.*, 2008). Three of these factors will be discussed: temperature, stimulation and chloride conductance (G_{Cl}). At 20-25°C maximal tetanic force, which represents the greatest possible force a muscle can generate, is unaffected between 4 and 7 mM K^+. It is reduced by 50% at 9 and 11 mM K^+ in soleus and EDL, respectively, and completely reduced to 0 at 12 mM K^+ (Fig. 1-8A) (Pedersen *et al.*, 2003;Cairns *et al.*, 1997). An increase in temperature to 35°C shifts the K^+-tetanic force relationship for soleus to higher $[K^+]_e$ such that 50% force depression occurs at 11 mM compared to 9 mM at 25°C (Fig. 1-8B).

Tetanic force is measured when the stimulation frequency produces multiple twitch contractions that fuse into tetani. Twitch force, on the other hand, is measured with a single stimulation causing a single action potential. Contrary to the K^+ effect on tetanic force, increasing $[K^+]_e$ up to 9 and 10 mM in soleus and EDL actually potentiates force by 10 to 20% at 25°C (Cairns *et al.*, 1997). Twitch potentiation at 37°C is even greater, being ~80%, and is observed at $[K^+]_e$ as high as 12-13 mM (Fig. 1-9). As of now, the

FIGURE 1-8

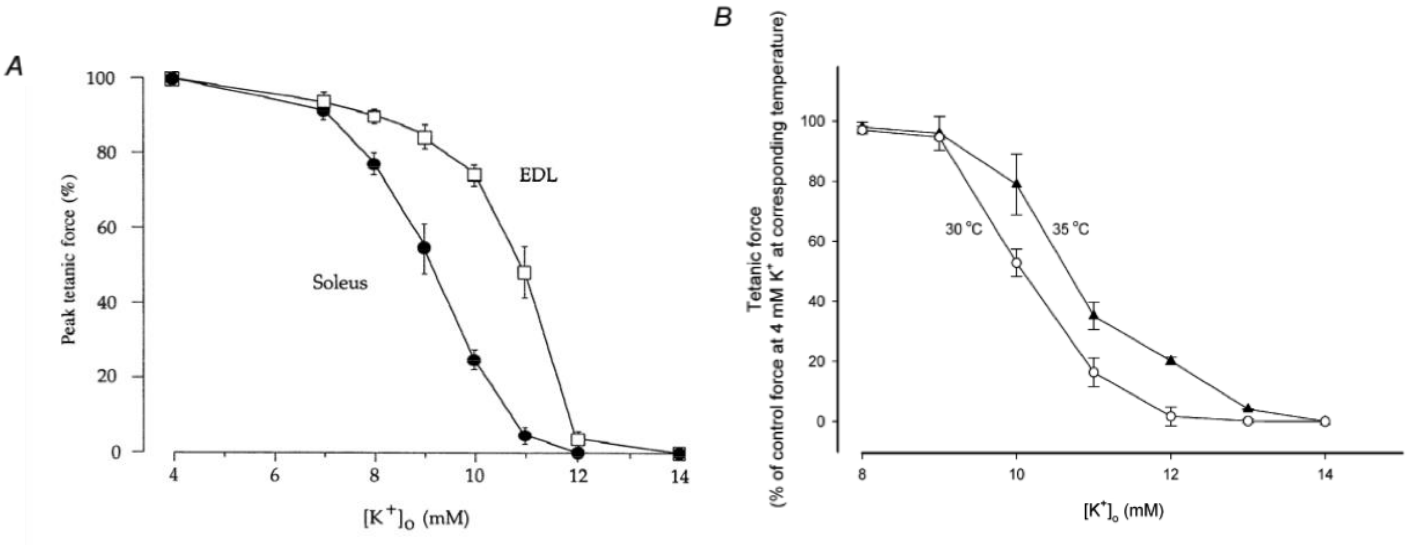

Figure 1-8. K^+-tetanic force relationships at different temperatures between 25 and 35°C. Effect of $[K^+]_e$ on peak tetanic force A) at 25°C in soleus and EDL when stimulated at 125 and 200 Hz, respectively; and in soleus at 30 and 35°C at 50 Hz. (Fig A from Cairns *et al.*, 1997 and Fig B from Pedersen *et al.*, 2003).

FIGURE 1-9

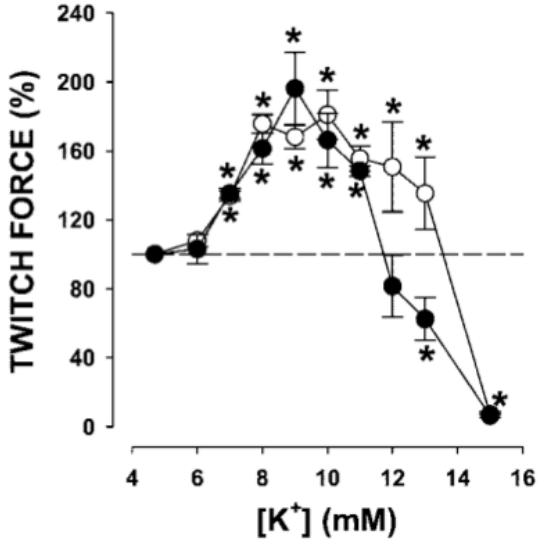

Figure 1-9. K^+-twitch force relationship at 37°C in EDL and soleus. Twitch force was elicited by a single stimulation of 0.3 ms duration and 8 V (Fig. from Yensen *et al.*,2002).

mechanism for this K^+-induced force potentiation is unknown. Twitch force depression occurs when $[K^+]_e$ exceeds 10-11 mM at 25°C and this concentration is shifted to 13-14mM at 37°C (Cairns *et al.*, 1997; Yensen *et al.*, 2002). Hence, the effect of K^+ on force generation is quite different between tetanic vs. twitch contractions, and at 25 vs. 35-37°C.

The apparent difference in the K^+-force relationship between EDL and soleus and with increases in temperature appears to be related to the changes in resting E_M with rising $[K^+]_e$. For a given $[K^+]_e$, soleus depolarizes more than EDL. For example at 25°C, a 10-fold increase in $[K^+]_e$ results in a 48 mV depolarization in EDL compared to a 51 mV depolarization in soleus (Cairns *et al.*, 1997). Similarly, as temperature increases, the extent of depolarization decreases although Yensen *et al.*, (2002) showed that the decrease in force occurs in the same E_M range at 25 and 37°C. Thus, the point at which K^+ depresses force seems to depend on resting E_M rather than the concentration of K^+. One reason for the different degree of depolarization in EDL vs. soleus and 25 vs. 37°C may be due to the level of Na^+-K^+ ATPase pump activity. For instance, activation of NKA pumps at high $[K^+]_e$ restores force and does so by repolarizing the membrane, allowing for recovery of membrane excitability (Pedersen *et al.*, 2003). Thus, the smaller depolarization and loss of force that occurs at 37°C and in EDL upon exposure to high $[K^+]_e$ is most likely due to a greater contribution from the NKA pumps (Yensen *et al.*, 2002;Pedersen *et al.*, 2003). A final important factor is the modulation of K^+ effects, which involves changes in chloride conductance.

CHLORIDE CONDUCTANCE

Conductance of an ion indicates its level of channel activity. In skeletal muscle,

Cl^- conductance (G_{Cl}) contributes 80-90% of the total resting membrane conductance, while the remaining 10-20% is contributed by K^+ via Kir2.1 and K_{ATP} channels (Pedersen *et al.*, 2009a;Kristensen *et al.*, 2004;Nielsen *et al.*, 2002). Cl^- has two main functions in the regulation of membrane excitability: 1) clamps resting membrane potential near -80 mV and 2) opposes the action potential depolarization phase and aids in the repolarization phase. For these reasons, Cl^- conductance is often referred to as "shunting" and inhibitory.

A shunt acts to stabilize an electrical potential by minimizing the influence of large electrical currents applied. Cl^- acts as a shunt because its activity reduces the influence of Na^+ and K^+ on the membrane potential. Consequently, if $[Cl^-]_e$ is reduced, the resting E_M during a train of action potentials or at high $[K^+]_e$ becomes more depolarized, increasing the inactivation of Na_V channels (Dulhunty, 1978;Cairns *et al.*, 2004). Furthermore, in the complete absence of $[Cl^-]_e$, the cell membrane depolarizes and causes repetitive action potentials long after stimulation has ceased. This is observed in Myotonia congenita, which is caused by loss-of-function due to mutations in the gene encoding for the ClC-1 Cl^-channel (Lehmann-Horn & Jurkat-Rott, 1999).

The Kir2.1 K^+ channels close during the action potential depolarization phase to prevent K^+ efflux and repolarization (Matsuda *et al.*, 1987). In contrast, the ClC-1 Cl^- channels, which also close during depolarization, have too slow kinetics and therefore remain open during the action potential (Fahlke *et al.*, 1998). Therefore, during the action potential, Cl^- moves inward and has an opposing influence on the Na^+-induced depolarization phase. At 4.7 mM K^+ the Cl^- conductance basically has no influence on action potential magnitude because the Na^+ conductance (G_{Na}) largely exceeds G_{Cl}

(Cairns *et al.*, 2004). However at high $[K^+]_e$, G_{Na} is reduced due to channel inactivation, while G_{Cl} remains unaffected. Consequently, the relative difference in G_{Na} and G_{Cl} decreases and the opposing influence of G_{Cl} becomes more prominent. At 9 mM K^+ depolarizes the membrane by 10 mV in EDL and reduces action potential overshoot by 15 mV, but reducing G_{Cl} by 50% re-established the large G_{Na}: G_{Cl} ratio and thereby improved action potential overshoot by 7mV (Fig. 1-10) (Pedersen *et al.*, 2005). Additionally, the reduction in G_{Cl} increased the amount of excitable fibers from 55 to 95% (Pedersen *et al.*, 2005). De Paoli *et al.*, (2013) also found that reducing G_{Cl} by decreasing $[Cl^-]_e$ from 127 to 60 mM improved excitability, action potential and force generation; but further reductions to 10 mM caused a severe depolarization in resting E_M, impaired action potential generation and reduced force. Thus, an optimal reduction in Cl^- of 60 mM was required to maintain force at high $[K^+]_e$. Sixty mM Cl^- was beneficial because its enhancing influence in increasing action potential generation was greater than its depolarizing effect on resting E_M. In contrast 10 mM Cl^- had the opposing effect as the depolarizing effect on resting E_M was greater than its beneficial effect on action potential generation. Two other studies also documented an improvement in contractile force at high $[K^+]_e$ when G_{Cl} was reduced by 30-60% (de Paoli *et al.*, 2010;Palade & Barchi, 1977). Thus these studies show that the reduction in Cl^- alleviates the K^+ sensitivity in muscle by shifting the $[K^+]_e$-force relationship to higher $[K^+]_e$.

OBJECTIVES AND HYPOTHESIS

Manipulating G_{Cl} pharmacologically could thus potentially provide alleviation for muscles afflicted by channelopathy diseases. The overall objective of this study was therefore to test the hypothesis that a reduction in G_{Cl} alleviates the K^+-induced paralysis

FIGURE 1-10

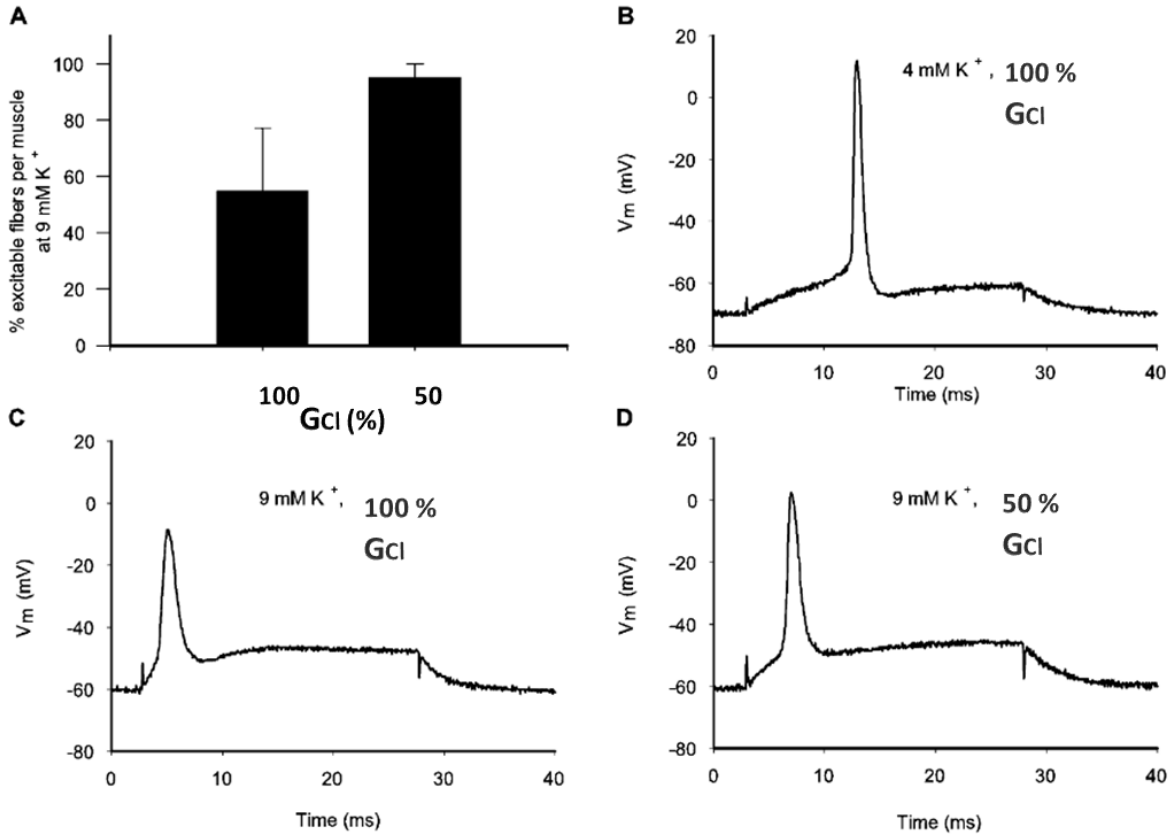

Figure 1-10. Effect of reducing G_{Cl} on action potential generation at high $[K^+]_e$ in rat soleus muscle. A) Amount of excitable fibers capable of generating an action potential upon stimulation at 9 mM K^+. B)-D) Representative action potentials at the indicated conditions. (Fig. adapated from (Pedersen *et al.*, 2005).

in HEPP by reducing K^+ sensitivity as it shifts the K^+-force relationship to higher $[K^+]_e$.

Previous studies on the K^+ and Cl^- effect have been carried out at 25 and 30°C and have used a narrow range of stimulation frequencies that are often not naturally occurring. Furthermore, when this study was started, it became obvious that the K^+ and Cl^- effects were not only temperature dependent, but also frequency dependent. **Aim 1** was to examine the K^+-force relationship and effect of reduced G_{Cl} at 37°C over a range of stimulation frequencies from twitch to full tetanus, which defines the type of force generated. This aim also became an important proof of principle regarding the Cl^- protective effects against K^+-induced force depression. **Aim 2:** Once the K^+ and Cl^- effects were clearly understood in wildtype, their effects were tested in HEPP.

MATERIALS AND METHODS

ANIMALS AND ETHICAL APPROVAL

All experiments were carried out using 1.5-2.5 month old female or male mice weighing 20-30 g. Animals were fed *ad libitum* and housed with 12 h light/dark condition, as according to guidelines of the Canadian Council for Animal Care (CCAC). All experimental procedures were approved by the Animal Care Committee of the University of Ottawa prior to any experiments. HEPP mice were generated by a knock-in of the human equivalent M1592V mutation. This means that a valine replaced a methionine at position 1585 into the SCN4A gene of the mouse [strain FVB.129S4(B6)-Scn4a$^{tm1.11Ljh}$/J], which is the same mouse strain used for wildtype (Hayward *et al.*, 2007). Homozygote HEPP mice do not survive past postnatal day five (Hayward *et al.*, 2007). So heterozygote HEPP mice were created by cross-breeding HEPP male mice with FVB1N female mice purchased from Charles River Laboratories, Canada. Mice were originally received from Dr. Lawrence Hayward at the University of Massachusetts Medical School, Worcester, Massachusetts. Mice were anaesthetized by intraperitoneal injection of 2.2 mg ketamine/0.4 mg xylazine/ 0.22 mg acepromazine per 10 g of animal body weight. Mice were then sacrificed by cervical dislocation.

GENOTYPING

DNA extraction was performed using a 2 mm tail piece. It was incubated overnight with 500 μL tail digestion buffer (0.2 mM disodium EDTA and 25 mM NaOH, pH 12.31) and 50 μL Proteinase K (1 mg/ml) at 56°C. DNA extraction involved the addition of 650 μL of 1:1 Phenol-CIA [chloroform-isoamyl alcohol (24:1 vol/vol)] and centrifugation at 12,000 *g* for 10 min at room temperature. Twice we added 650 μL of

CIA to the pellet and centrifuged for 10 min before suspending the resulting pellet in 750 μL of isopropyl alcohol. The solution was then centrifuged 15 min at 15, 000 *g*. The alcohol was removed, and the pellet was suspended in 750 μL of 70% ethanol and centrifuged. After the alcohol was removed, the pellet was left to dry for 30 min prior to addition of 200 μL 1X TE buffer (10 mM Tris, 1 mM EDTA, pH 8.0), and incubated for two h at 65°C. PCR was then completed on the previously extracted DNA. The following two primers were used: NC1F (forward): 5'TGT CTA ACT TCG CCT ACG TCA A 3'; NC2R (reverse): 5' GAG TCA CCC AGT ACC TCT TTG G 3'.

PCR products were digested for 6 h with the restriction digest enzyme *NspI*. The mutation that is knocked in for HEPP mice causes the removal of one *NspI* cut site that is easily detected by agarose gel electrophoresis. Two bands are visualized for wild-type, which carry the cut site on both alleles, while three bands are seen for heterozygous HEPP mice that contain one normal allele and one mutant allele.

MUSCLE AND SOLUTIONS

All contractility and electrophysiological experiments were performed in vitro using isolated EDL or soleus muscles. EDL is a fast-twitch muscle primarily composed of type IIB and IIX fibers; soleus is a slow-twitch muscle primarily composed of type I and IIA fibers (Banas *et al.*, 2011).

All muscles were initially superperfused in a physiological solution containing in mM: 118.5 NaCl, 4.7 KCl, 1.3 $CaCl_2$, 3.1 $MgCl_2$, 25 $NaHCO_3$, 2 NaH_2PO_4, and 5.5 g D-glucose (control solution). Solutions were continuously gassed with a mixture of 95% O_2: 5% CO_2 (~pH 7.4) throughout the experiment. Solutions with reduced $[Cl^-]_e$ were prepared by replacing the appropriate amount of NaCl with sodium methanesulfonate.

Solutions containing anthracene-9-carboxylic acid (9-AC), a Cl^- channel blocker, were prepared by dissolving the desired amount of 9-AC in 0.1% DMSO (vol/vol). Experimental temperature was 37°C.

FORCE MEASUREMENT

Muscles were mounted horizontally into a chamber and attached to a force transducer at one end (Model #400A, Aurora Scientific, Canada), and to a stationary hook at the other end. Physiological solution entered the chamber just below and above the muscle at a constant rate of 15 ml/min. Force transducers were connected to a KCP13104 data acquisition system (Keithley, USA) and data sampling was obtained at 5 kHz. Parameters of the contraction were later obtained with a computer analysis program. Peak force was defined as the force generate by electrical stimulation and calculated as the difference between maximum force during stimulation and baseline force measured 5 msec before stimulation.

STIMULATION

Contractions were evoked every 10 min by field stimulation using two platinum wires. They were connected to a Grass S88 stimulator and a Grass SIU5 isolation unit (Grass Technologies, USA). Stimulations were square pulses of 0.3 msec duration given at supra-maximal voltage (10V) and at a frequency varying according to the experiment.

ELECTROPHYSIOLOGICAL MEASUREMENTS

The muscle chamber, solutions and muscle stimulation were all as described for the measurement of force. Membrane potentials were measured using conventional microelectrodes as described by (Matar *et al.*, 2000) Briefly, microelectrodes (with tip potentials <5 mV and tip resistance varying from 3 to 8 MΩ) and reference electrodes

(tip resistance of 1 MΩ) were filled with 2 M potassium acetate. Action potentials were elicited by passing a small current between two platinum wires placed along the surface fibers to stimulate a small number of fibers. Action potentials were digitized at a sampling rate of 200 kHz. Resting membrane potential was measured from the baseline of the action potential.

EXPERIMENTAL PROTOCOL

At the beginning of each experiment, muscles were optimally lengthened to give maximum peak force while they were stimulated every 3 min. Once maximum force was obtained, muscles were allowed a 30 min equilibrium period, while being stimulated every 10 min. The equilibrium period ensured that a muscle was stable, and a muscle was discarded only for wildtype if force loss was greater than 10%. At the end of the equilibrium period, muscles were then exposed to the various testing conditions of high $[K^+]_e$, low $[Cl^-]_e$ or 9-AC. Once measurements were completed, the control solution was reintroduced to determine reversibility of the various test conditions.

STATISTICS

All data are expressed as means ± S.E. Split-plot ANOVA was used to determine significant differences. ANOVA calculations were made using Statistical Analysis Software (SAS Institute Inc., Cary, NC, USA). When a main effect or interaction was significant, the least square difference (LSD) was used to locate the significant differences. The word "significant" refers only to a statistical difference ($P < 0.05$).

RESULTS

Stimulation of isolated mouse skeletal muscle conducted at physiological temperature (37°C) can significantly reduce contractile force. A major reason for the force loss is not the development of a hypoxic core at the center of the muscle, but an increase in reactive oxygen and nitrogen species (ROS, RNS) (Barclay, 2005;Edwards *et al.*, 2007). This problem was addressed in the current study by using a superperfusion system (see Materials & Methods) allowing for quick waste removal. Thus, over the span of a 2-hour experiment, wildtype EDL and soleus muscles never lost more than 15% of peak force under control conditions (data not shown). However, when extracellular K^+ ($[K^+]_e$) was raised, impairment of contractility occurred for EDL muscles when stimulated every 100 sec, a time initially used in many studies by Renaud & colleagues. For example, at 10 mM K^+, EDL peak force decreased by 40% over 50 min and barely recovered upon return to 4.7 mM K^+ (Fig. 3-1). In comparison, contractions elicited every 5 or 10 min only resulted in a 10% loss of peak force over 50 min, for which there was no impairment during recovery back to 4.7 mM K^+. Therefore, all further experiments utilized at least a 5 min stimulation interval rather than a 100 sec interval.

K^+-FORCE RELATIONSHIP IN WT EDL & SOLEUS

TWITCH

Twitch contractions are the result of one supramaximal stimulation that generates a single action potential. At 4.7 mM K^+, wildtype EDL generated mean peak twitch force of 3.2 N/cm^2 and remained unchanged for up to 2 hrs (Fig. 3-2A). Raising $[K^+]_e$ from 4.7 to 8 mM resulted in a significant and progressive increase in peak twitch force, reaching 175% in 2 hrs. Potentiation of twitch force was much more rapid at 13 mM K^+ for which

FIGURE 3-1

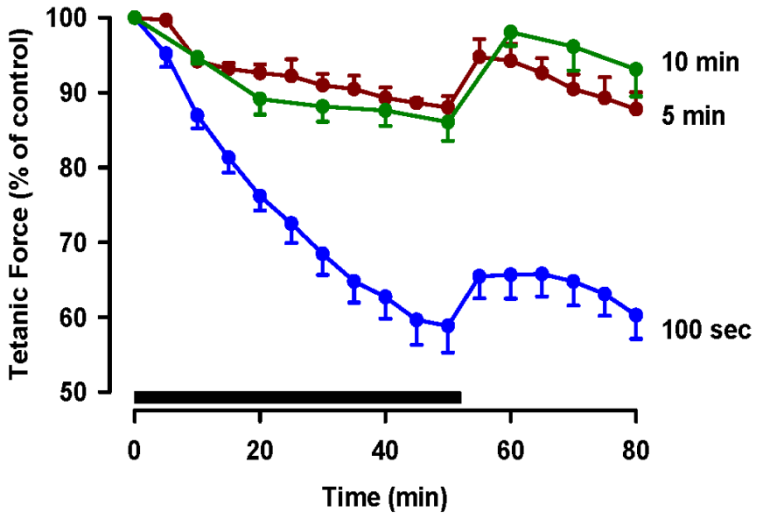

Figure 3-1. Wildtype EDL muscles were most stable if the contraction interval was 5 or 10 min. At time 0 min, $[K^+]_e$ was increased from 4.7 mM to 10 mM K^+ for 50 min. The time indicated at the end of each curve represents the time interval between contractions. Tetanic contractions were 200 msec long at a stimulation of 200 Hz. A 20 min recovery period followed at 4.7 mM K^+. Symbol: black bar, exposure to 10 mM K^+. Vertical bars represent S.E. of 2-5muscles.

FIGURE 3-2

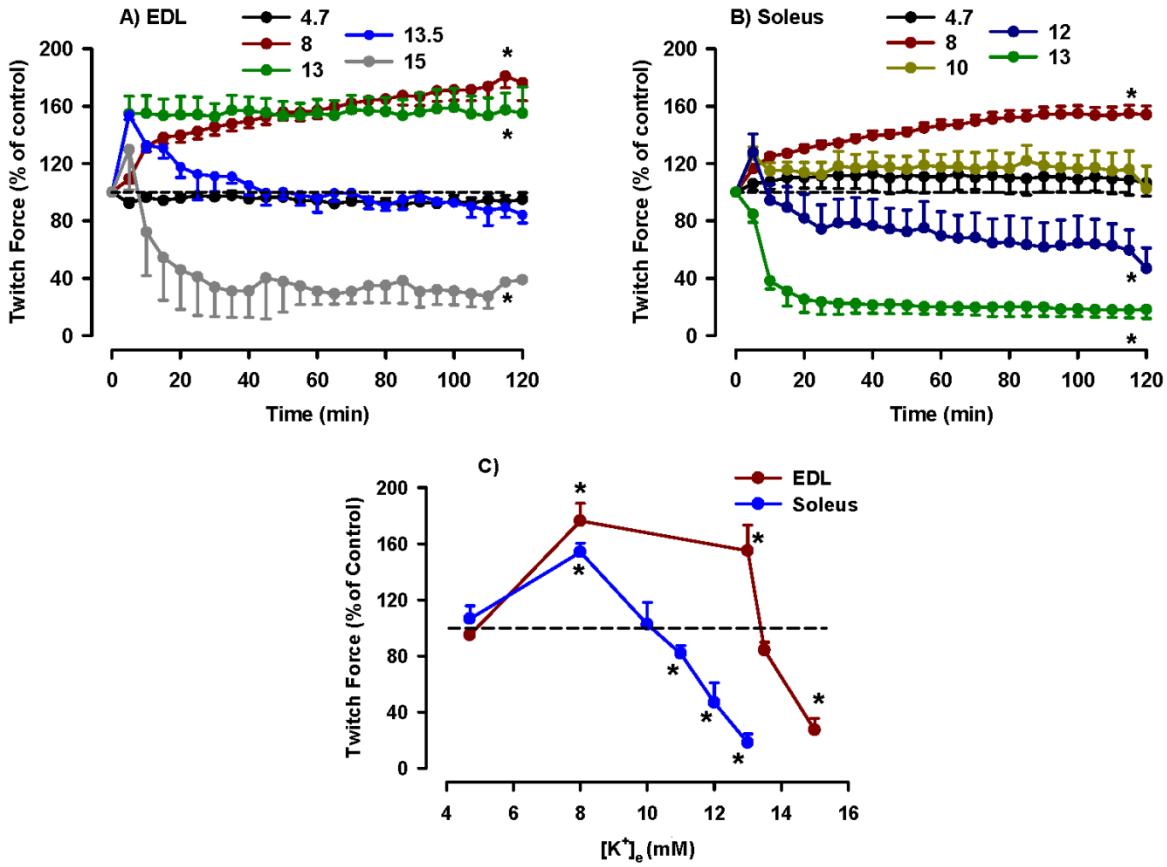

Figure 3-2. $[K^+]_e$-Peak twitch force relationship. Changes in twitch force overtime following increases in $[K^+]_e$ in A) EDL and B) soleus**.** Muscles were stimulated every 5 min. $[K^+]_e$ was raised at time 0 min to the indicated concentration (in mM). Twitch forces are expressed as a percent value of the force at time 0. C: K^+-force relationship using the percent values at 120 min. The dotted line represents 100% force. Vertical bars are S.E. for 2-11 muscles.

* Significantly different from mean peak twitch force at 4.7 mM K^+

ANOVA, L.S.D. $P<0.05$

a steady-state of 153% was reached within 5 min. A further increase to 13.5 mM K^+ resulted in a transient potentiation, followed by a continuous decline in force. At 15 mM K^+, twitch force again transiently increased , followed by a decrease to 27% by 40 min.

At 4.7 mM K^+, wildtype soleus generated mean peak twitch force of 1.1 N/cm^2 and increased by 10% over a 2 hr period (Fig. 3-2B). Like the EDL, raising $[K^+]_e$ to 8 mM resulted in a progressive and significant increase in twitch force to 160%, but for which steady-state was achieved by 80 min. At 10 mM K^+, there was no significant increase in force , while, 13 mM K^+ potentiated twitch force in EDL, but significantly decreased twitch force in soleus.

The force measured at 120 min was used to document the K^+-twitch force relationship (Fig. 3-2C). Twitch force was significantly potentiated in EDL at 8 and 13 mM K^+ and in soleus at 8 mM K^+. Twitch force was not significantly reduced until the K^+ concentration was 11 and 15 mM K^+ for soleus and EDL, respectively.

TETANUS

Tetanic contractions are produced when the stimulation frequency is increased and multiple twitches fuse. While a single twitch generates 1-3 N/cm^2, increasing the frequency up to 100 Hz produced a peak force of 8-10 N/cm^2 (Fig. 3-3A). However, at that frequency an unfused tetanus occurred in EDL, whereby part of the individual twitches could still be observed. By 160 Hz, the contractions appeared almost completely fused and by 200 Hz peak tetanic force was 20 N/cm^2. Similarly in soleus, increasing the stimulation frequency up to 50 Hz resulted in an unfused tetanus (Fig. 3-3.B). A fused tetanus was observed at 100 Hz, a lower frequency than in EDL. The peak force measured during a stimulation of 200 Hz for EDL and 140 Hz for soleus represented the

FIGURE 3-3

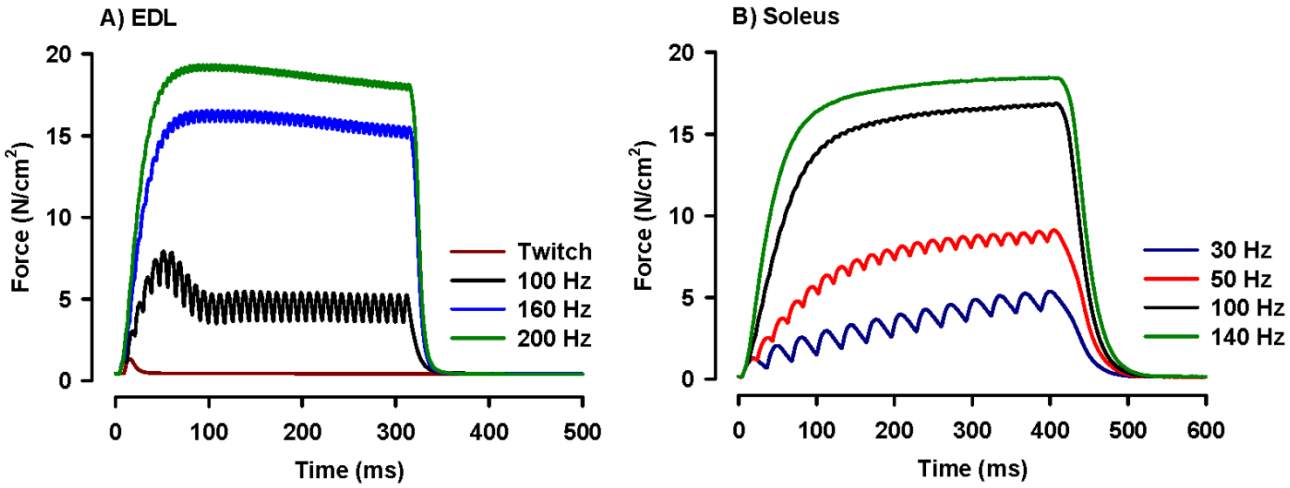

Figure 3-3. Representative traces of contractions at various stimulation frequencies. Stimulation durations were for 300 ms in EDL and 400 ms in soleus. Individual twitches are still visible with sub-maximal frequencies (unfused), but are not visible with maximal frequencies (fused).

maximum force a muscle could generate and here is referred to as the peak tetanic force (Fig. 3-4).

At 4.7 mM K^+, mean peak tetanic force of wildtype EDL was 26.7±1.4 N/cm^2. At 4.7 mM K^+, force declined by 7% during the 50 min. In contrast to twitch force, elevating $[K^+]_e$ never potentiated tetanic force. For EDL, force slowly declined at 11 mM K^+, although not significant, to a new steady-state of 88% by 40 min (Fig. 3-4.A). The decline in force was significant by 13.5 mM K^+. At 14 and 15 mM K^+, force was drastically reduced to 20% within 50 min. Upon a return to 4.7 mM K^+, all peak tetanic forces increased back to that observed for muscles kept at 4.7 mM K^+ for the whole experiment.

In wildtype soleus, mean peak tetanic force at 4.7 mM K^+ was 15.3±0.9 N/cm^2. Force loss overtime while keeping $[K^+]_e$ at 4.7 mM was 5% by 50 min (Fig. 3-4.B). Raising $[K^+]_e$ to 10 mM K^+ decreased force to 80% within 10 min. The reduction in force was significant at 11 mM K^+, to 65% within 35 min. By 12 and 13 mM K^+ force was reduced to 35 and 23%, respectively.

The force measured at 50 min was used to document the K^+-tetanic force relationship (Fig. 3-4.C). For EDL, there was no decrease in tetanic force up to 11 mM, which then decreased to 75% by 13 mM and to 20% by 15 mM. For soleus, there was no decrease in tetanic force up to 8 mM, which then decreased to 65% at 11 mM and to 35% at 12 mM. As observed for twitch, tetanic force in soleus was more sensitive to K^+, exhibiting a lower critical $[K^+]_e$ of 8 mM compared to 13 mM in EDL.

EFFECT OF K^+ ON FORCE AT LOW STIMULATION FREQUENCIES

As mentioned in the Introduction, twitch and maximal tetanic contractions

FIGURE 3-4

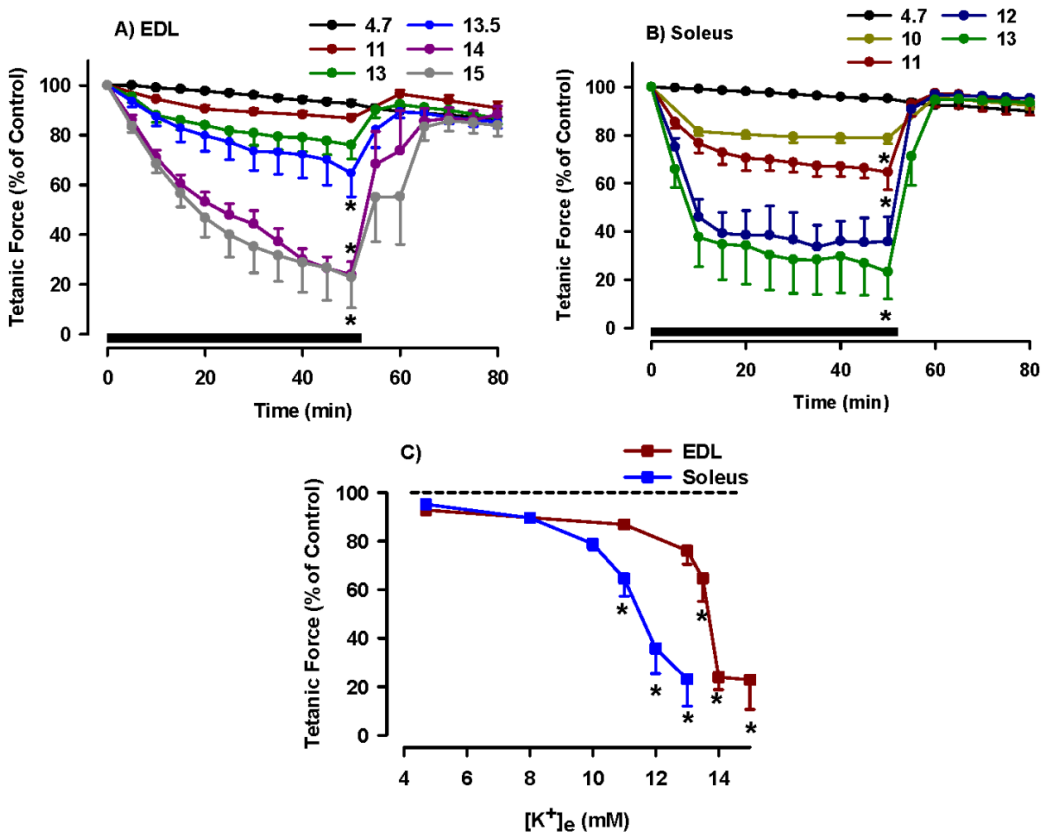

Figure 3-4. $[K^+]_e$-Peak tetanic force relationship. Changes in tetanic force overtime following increases in $[K^+]_e$ for A) EDL and B) soleus. Muscles were stimulated every 5 min at 140 Hz for soleus and 200 Hz for EDL. Stimulation durations were 200 msec for EDL and 300 msec for soleus. $[K^+]_e$ was increased (in mM) at time 0 min for 50 min at the indicated concentrations. Black bar: exposure to high K^+. Tetanic forces are expressed as a percent of the force at time 0. C) K^+-force relationship using the percent values at 50 min. Vertical bars represent the S.E. of 4-5 muscles.

* Significantly different from mean peak tetanic force at 4.7 mM K^+

ANOVA, L.S.D. $P<0.05$.

are rare occurrences as most of the time soleus is stimulated between 30-50 Hz and EDL between 90-100 Hz (Hennig & Lomo, 1985). Thus, for this study, the K^+ effect was tested at stimulation frequencies from 10 to 200 Hz. To do this rapidly, peak force was measured at different frequencies between 1 (twitch) and 200 Hz, first at 4.7 mM K^+ and then for a second time at high K^+ once a steady-state was achieved. Between 1 and 50 Hz at 4.7 mM K^+, force generated by EDL was less than 10% of peak tetanic force (Fig. 3-5A). Increasing the stimulation frequency to 100 and 140 Hz augmented peak force to 31% and 70%, respectively. When the peak force generated at 8 mM K^+ was expressed as a percent of the force at 200 Hz and 4.7 mM K^+, a potentiation became apparent at the lower frequencies between 1 and 140 Hz, while a force depression only occurred at 200 Hz. At 4.7 mM K^+, soleus peak force was also less than 10% of peak tetanic force when stimulated between 1 and 30 Hz. By 50 and 100 Hz, peak force was 35% and 90%, respectively (Fig. 3-5.B). By 140 Hz, peak tetanus force was generated. Soleus also generated greater force at lower stimulation frequencies when $[K^+]_e$ was raised to 8 mM. However, force potentiation occurred in a narrow range; i.e., between 1 and 50 Hz, compared to 1 and 150 Hz in EDL.

To better view the extent of the potentiation at various frequencies, the force at each frequency measured at high $[K^+]_e$ was expressed as a percent of the force measured at 4.7 mM K^+. For one group of muscles, $[K^+]_e$ was kept at 4.7 mM K^+ for the entire experiment. For these EDL muscles, the difference in peak force was less than 5% between the first and second measurement (Fig 3-6A). Increasing $[K^+]_e$ to 8 mM resulted in a potentiation of force between 1 and 140 Hz with the greatest increase to 155% occurring at 50 Hz. At 140 Hz, force was potentiated by 16% and decreased. to 93% at

FIGURE 3-5

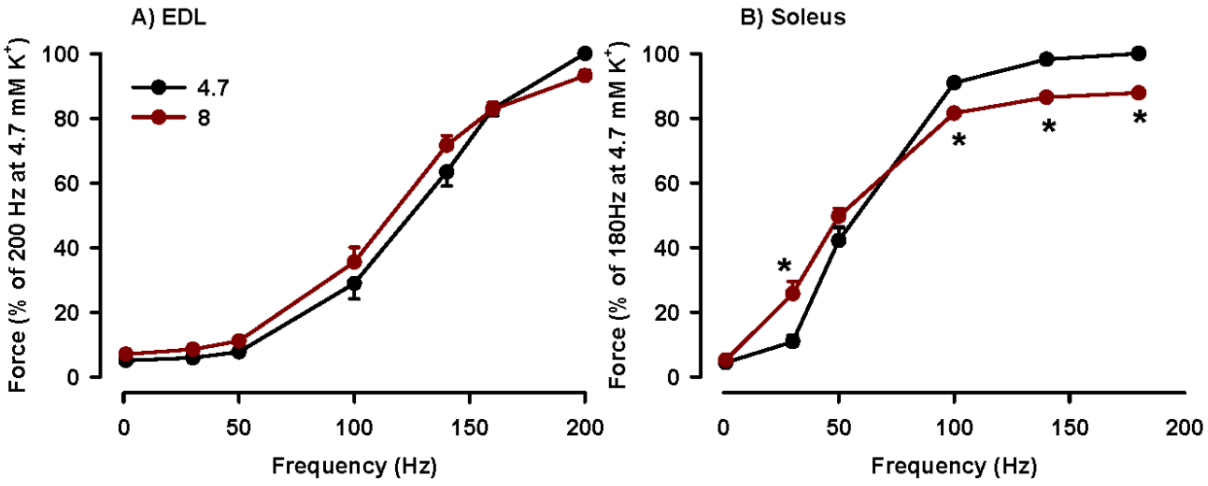

Figure 3-5. Eight mM K^+ potentiated force at low frequencies while it depressed force at high frequencies in A) EDL and B) soleus. The first force-frequency was conducted at 4.7 mM K^+ and then K^+ was increased to 8 mM for 2 hr while twitch contractions were elicited every 5 min. A second force-frequency was conducted at 8 mM K^+. For the force-frequencies, stimulation duration used was 300 msec for EDL and 400 msec for soleus. Force was calculated as a percent of the peak tetanic force measured at 4.7 mM K^+. Vertical bars represent S.E. for 6 muscles

* Significantly different from mean force at 4.7 mM K^+ for the same frequency

ANOVA, L.S.D. $P<0.05$

FIGURE 3-6

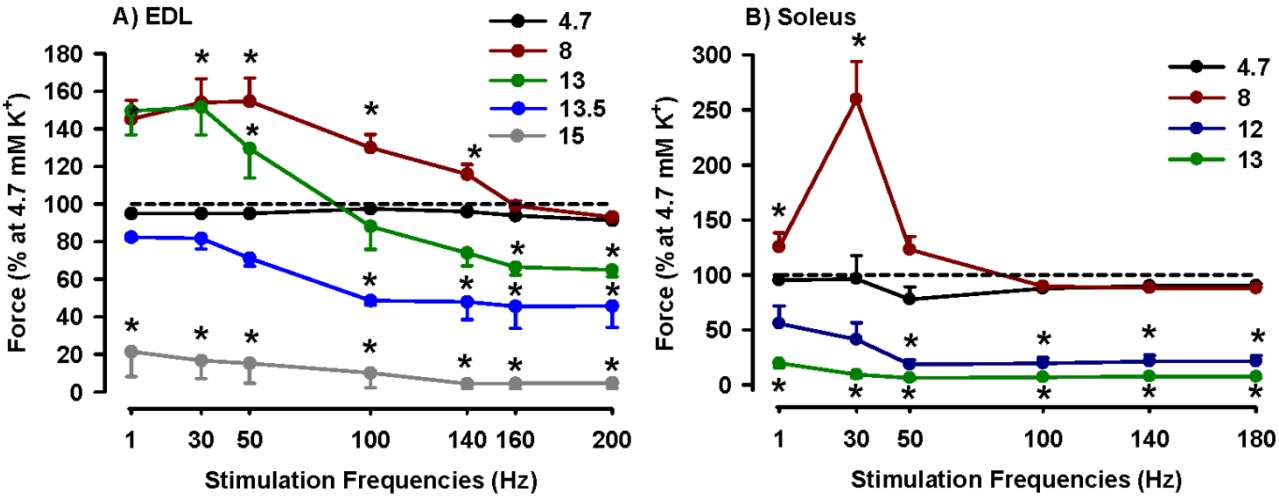

Figure 3-6. Peak K^+-induced force potentiation occurred in muscles stimulated at low frequencies. Peak force at different frequencies was first measured at 4.7 mM K^+. K^+ was either kept at 4.7 mM or increased to the indicated concentration (in mM) for 2 hr. A second series of force measurements were then repeated. For each stimulation frequency, the forces from the second measurements were calculated as a percent of the force measured the first time. Vertical bars represent S.E. for 2-6 muscles.

* Significantly different from mean peak force at 4.7 mM K^+ for the same frequency ANOVA, L.S.D. $P<0.05$

200 Hz. The extent of potentiation at 13 mM was similar to that at 8 mM, but only occurred between 1 and 50 Hz. By 160 and 200 Hz force was significantly reduced by 45%. At 13.5 mM K^+, force was significantly reduced by 50% from 100 to 200 Hz. Force was further depressed upon exposure to 15 mM K^+ by more than 80% at all frequencies. K^+-induced force potentiation was more restricted in soleus (Fig 3-6B). Like for EDL, 8 mM K^+ potentiated force at lower frequencies, but only between 1 and 50 Hz, including a significant potentiation to 260% at 30 Hz. Whereas 13 mM K^+ still enhanced force in EDL at lower frequencies, force was depressed by 12 mM in soleus and severely depressed to <10% between 30-180 Hz at 13 mM K^+.

MODULATION OF THE K^+-FORCE RELATIONSHIP BY CHLORIDE

As mentioned in the introduction, a decrease in G_{Cl} can improve force at elevated $[K^+]_e$, but is still unknown at which frequency this occurs at 37°C. G_{Cl} was reduced using two protocols: 1) lowering the Cl^- in the solution ($[Cl^-]_e$) to reduce the Cl^- concentration gradient and thus current; and 2) incubating muscle with 9-anthracene-carboxylic acid (9-AC), a ClC-1 Cl^- channel blocker.

LOW CHLORIDE SOLUTION

Initially the aim was to conduct the Cl^- experiments at a $[K^+]_e$ that caused a ~50% force loss because at higher K^+ concentrations the force loss may be too severe for significant force recovery even at a stimulation frequency that normally occurs in vivo. Thus, a concentration of 13 mM K^+ was chosen for EDL as it caused a 50% depression of force at 90 Hz, and 12 mM K^+ at 30 Hz for soleus. For the soleus, 12 mM K^+ caused a 55% depression in peak force (Fig. 3-7B), a value similar to that shown in Fig. 3-6B. However, the force depression in EDL at 13 mM K^+ at 90 Hz was much greater in this

FIGURE 3-7

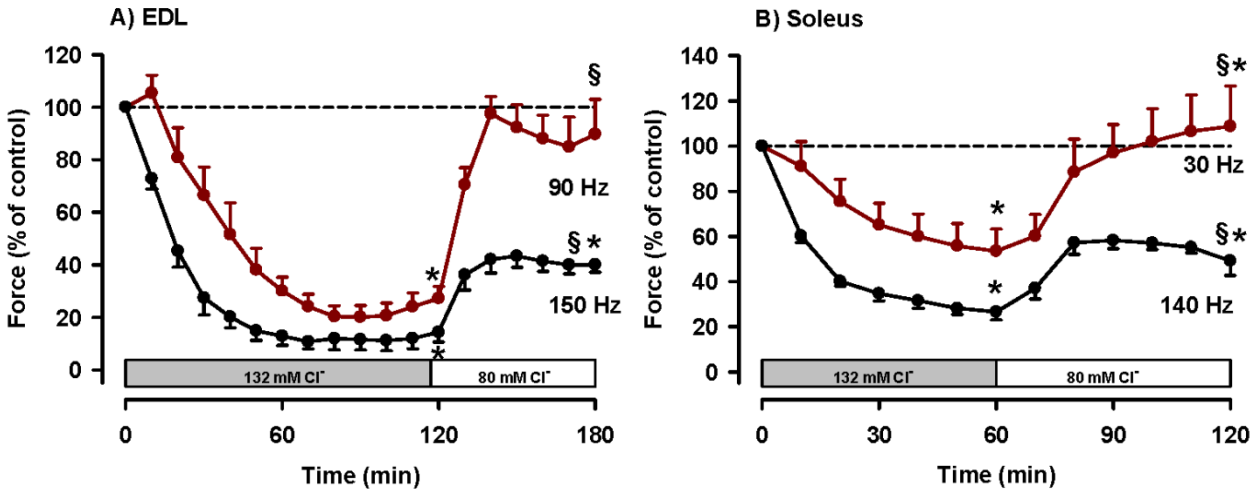

Figure 3-7. Time courses showing the recovery of force at low $[Cl^-]_e$ during an exposure to high K^+ in A) 13 mM for EDL and B) 12 mM for soleus. $[K^+]_e$ was increased at time 0 min for the entire experiment. Contractions were elicited with 2 sec train of pulses at the indicated frequency. Vertical error bars represent S.E. for 4-5 muscles.

* Significantly different from mean peak force at time 0

§ Significantly increased upon reducing $[Cl^-]_e$ from 132 to 80 mM

ANOVA, L.S.D. $P<0.05$

series of experiments, as the force decreased by 80% (Fig. 3-7A) as opposed to 50% at 100 Hz in the previous experiments (Fig. 3-6A).

Regardless of the decrease in force by K^+, reducing $[Cl^-]_e$ from 132 to 80 mM alleviated the depressive effects of high $[K^+]_e$ in both EDL and soleus. For EDL at 13 mM K^+, peak force at 90 Hz re-increased from 25 to 90%, representing a 65% difference (Fig. 3-7A). Experiments were also done at 150 Hz, at which the recovery was much smaller, i.e. 30%, but still significant. For soleus at 12 mM K^+, the reduction in Cl^- at 30 Hz allowed for a significant recovery and potentiation of force to 108%. Like for EDL, stimulating at a higher frequency of 140 Hz resulted in a smaller, but still significant recovery to 50% (Fig. 3-7B).

In a second series of experiments, lower $[K^+]_e$ were used and was chosen using a range that already potentiated force. For EDL, an exposure to 10 mM K^+ increased peak force at 90 Hz by 15%, which was then significantly increased to 154% when Cl^- was reduced from 132 to 80 mM while $[K^+]_e$ remained at 10 mM (Fig. 3-8A). For soleus, the initial increase at 10 mM reached 177% and increased further to 243% when Cl^- was reduced to 80 mM (Fig. 3-8B). Returning to normal conditions, force decreased to 80% of control, which was not significantly different than the original peak tetanic force.

When stimulated at 90 Hz, EDL force was significantly improved by the reduction in Cl^- to 80 mM, increasing by 60-70% at both $[K^+]_e$ tested. This effectively shifted the EDL K^+-force relationship to higher $[K^+]_e$, as the critical $[K^+]_e$ required to depress force was shifted from 11 mM K^+ in 132 mM Cl^- solution to 13 mM K^+ in 80 mM Cl^- solution. Similar to EDL, soleus displayed a 50-60% improvement in force at both $[K^+]_e$ tested, but only when stimulated at a lower frequency of 30 Hz. Thus, the

FIGURE 3-8

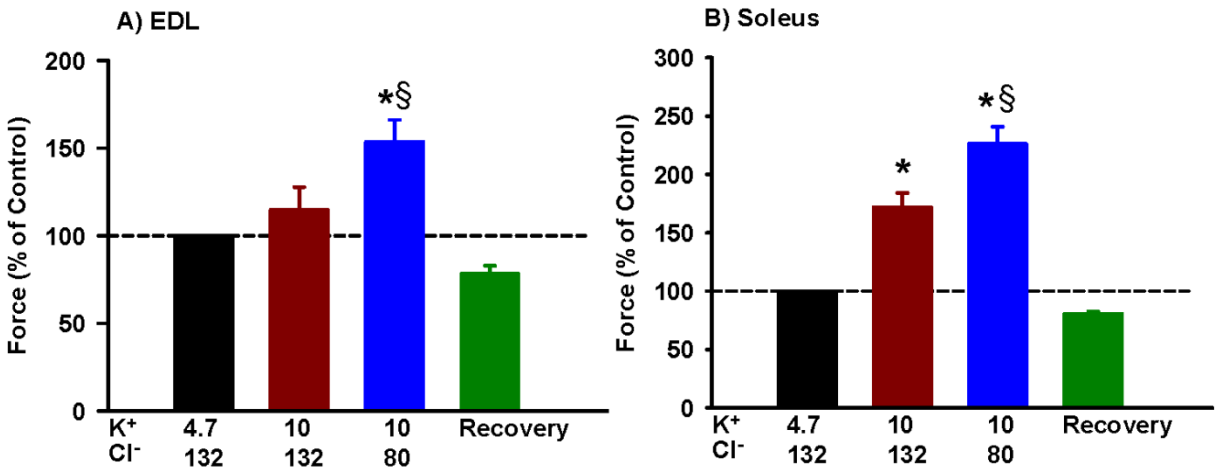

Figure 3-8. Low $[Cl^-]_e$ improved force potentiation during an exposure to 10 mM K^+. Muscles were exposed to 10 mM K^+ for 2 hr before Cl^- was reduced. Values were taken at 60 min of low Cl^- incubation. Recovery involved returning back to the solution containing 4.7 mM K^+ and 132 mM Cl^-. Two sec stimulation duration was used while stimulation frequency used was 90 Hz in EDL and 30 Hz in soleus. Vertical error bars represent S.E. for 2-3 muscles.

* Significantly different from mean peak force at 4.7 mM K^+

§ Significantly increased upon reducing $[Cl^-]_e$ from 132 to 80 mM

ANOVA, L.S.D. $P<0.05$

reduction in Cl^- from 132 to 80 mM shifted the soleus K^+-force relationship to higher $[K^+]_e$, as the critical $[K^+]_e$ increased from 11 mM to 12 mM K^+.

9-ANTHRACENECARBOXYLIC ACID (9-AC)

To estimate the optimal Cl^- conductance (G_{Cl}) that allowed for the best improvement of force at high $[K^+]_e$, the extent of recovery upon exposure to several different 9-AC concentrations was examined. According to a dose-response curve obtained from diaphragm muscles from rats (Palade & Barchi, 1977), the 9-AC concentrations of 6.5, 12, 20, 38 and 100

μM should reduce G_{Cl} by 30, 50, 70, 90 and 100%, respectively.

EDL muscles were first exposed to 13 mM K^+ for 60 min, which decreased force to 20-30% of the force at 4.7 mM K^+ (Fig. 3-9A). The addition of 6.5, 12 and 20 μM 9-AC was followed within 10 min by a force recovery of 23%, 39% and 42%, respectively. There were no significant changes in force thereafter at those 3 concentrations. Thirty-eight μM and 100 μM 9-AC provided the most significant recovery over a 10 min period. However, while the initial force recovery at 38 and 100 μM were the greatest, it was only transient as force rapidly decreased back to lower values. The situation was quite similar with soleus muscles, which were tested at 12 mM K^+. The addition of either 6.5, 12 or 20 μM 9-AC did not significantly restore force. With 38 and 100 μM, force rapidly decreased after an initial recovery (Fig. 3-9B). It appears that over the 1 hr 9-AC incubation period, the optimal [9-AC] for force recovery were 20 and 38 μM for EDL and soleus, respectively (Fig. 3-9C, D). According to the dose-response curve, this would correspond to a 70 and 90% reduction in G_{Cl} for EDL and soleus.

FIGURE 3-9

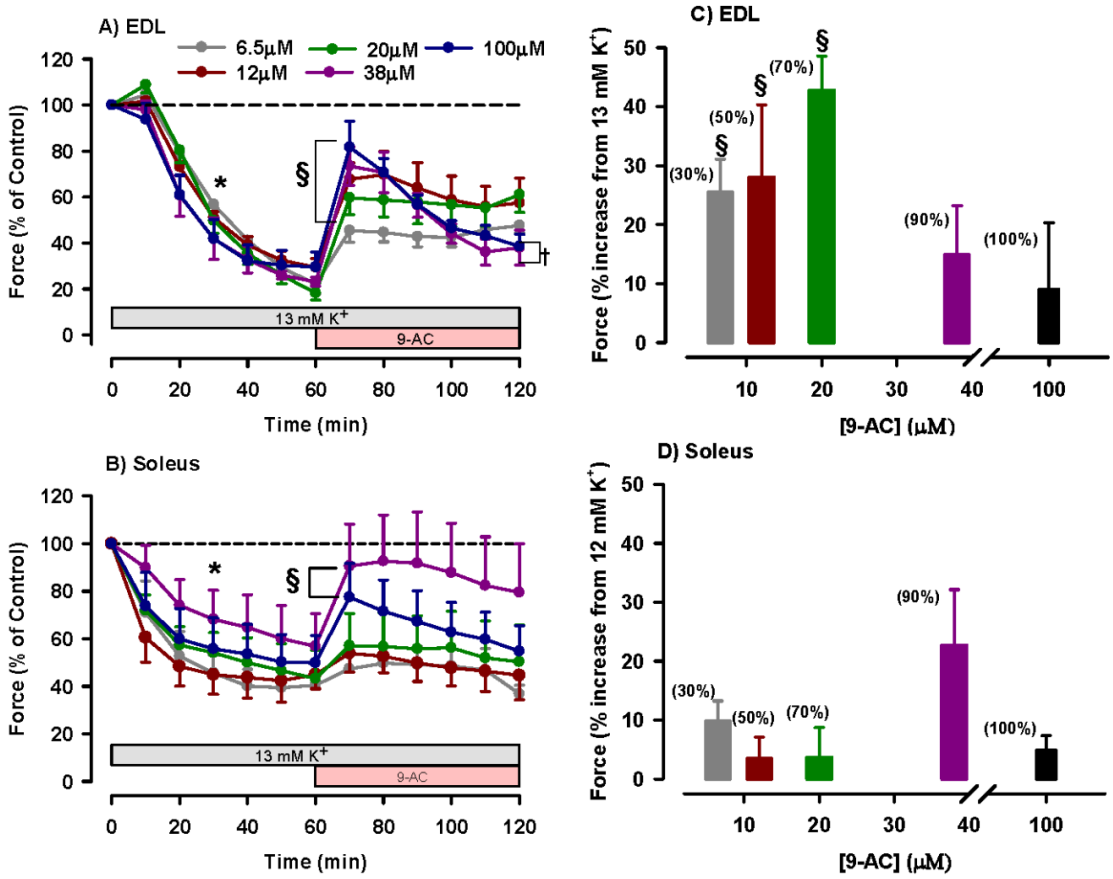

Figure 3-9. Reducing G_{Cl} with 9-AC allowed for force recovery during an exposure to high $[K^+]_e$ at A) 13 mM for EDL and B) 12 mM for soleus. Muscles were incubated in high $[K^+]_e$ at 0 min for the entire experiment. At 60 min, 9-AC was added to the solution for 1 hr. Stimulation frequency was 90 Hz in EDL and 30 Hz in soleus. Two sec train of pulses were applied every 10 min. Dose-response curves for C) EDL and D) soleus were created by taking the mean peak forces at 120 min subtracted from the mean peak force at 60 min prior to the addition of 9-AC. The percent values are estimate reductions in G_{Cl} taken from the study of Palade & Barchi, (1977). Vertical error bars represent S.E. for 4-5 muscles.

* All peak forces at high K^+ became significantly reduced by 30 min

§ Significantly increased upon adding 9-AC

†Force after the initial increase in the presence of 9-AC significantly decreased

ANOVA, L.S.D $P<0.05$

K^+ AND Cl^- EFFECTS ON MEMBRANE EXCITABILITY

As mentioned in the Introduction, the maintenance of membrane excitability is important for the capacity to generate force and the direct effects of changing $[K^+]_e$ and $[Cl^-]_e$ is on the resting E_M. For EDL, mean resting E_M at 4.7 mM K^+ was -77 mV (Fig. 3-10A). Increasing $[K^+]_e$ to 9 and 11 mM depolarized the cell membrane to -64 and -61 mV, representing a 43 mV depolarization per 10-fold increase in $[K^+]_e$. When $[Cl^-]_e$ was reduced from 132 to 80 mM at 11 mM K^+, resting E_M repolarized from -61 to -62 mV, which was not statistically significant. For soleus, mean resting E_M was -72 mV (Fig. 3-10B). Increasing $[K^+]_e$ to 9 and 11 mM depolarized the cell membrane to -59 and -56 mV, representing a 43 mV depolarization per 10-fold increase in $[K^+]_e$ as well. Reducing $[Cl^-]_e$ to 80 mM caused a significant repolarization of the cell membrane from -59 to -61 mV at 9 mM K^+. As expected from other studies, the K^+-induced depolarization resulted in significantly lower action potential overshoot. For EDL, mean action potential overshoot at 4.7 mM K^+ was 20 mV (Fig. 3-10C). Increasing $[K^+]_e$ to 9 and 11 mM reduced the overshoot to 9 and 5 mV, respectively. When $[Cl^-]_e$ was reduced to 80 mM, overshoot improved to 8 mV at 11 mM K^+, but with 20 mM Cl^-, overshoot decreased to -3 mV. For soleus, mean action potential overshoot at 4.7 mM K^+ was 21 mV (Fig. 3-10D). Increasing $[K^+]_e$ to 9 and 11 mM reduced the overshoot to 8 and 3 mV, respectively. When $[Cl^-]_e$ was reduced to 80 mM, action potential overshoot improved significantly from 8 to 14 mV at 9 mM K^+, but was reduced to -2 mV at 20 mM Cl^-. Returning to control conditions allowed for full recovery of resting E_M to -75 and -70 mV in EDL and soleus, respectively. Overshoot also recovered in EDL to 21 mV and in soleus to 16 mV. The number of excitable fibers was also documented, defined here as the number of tested fibers that generated an action potential upon stimulation. Although not statistically

FIGURE 3-10

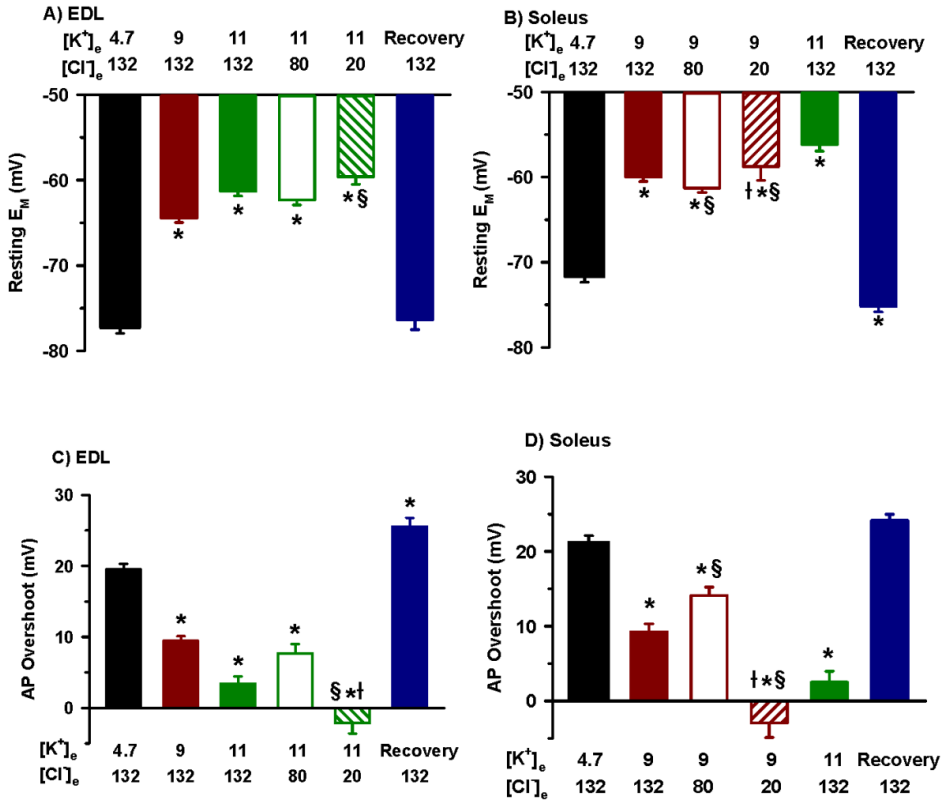

Figure 3-10. High $[K^+]_e$ depolarized resting E_M and decreased action potential (AP) overshoot. Action potentials were measured from fibers at the muscle surface for each condition after a 20 min incubation period. This ensured enough time for the E_M of surface fibers to reach a new steady state. Vertical error bars represent S.E. for 5-8 muscles (for a total of 30-48 fibers at each condition).

* Significantly different from resting E_M and AP overshoot at 4.7 mM K^+

§ Values at high K^+/low Cl^- are significantly different from the values at high K^+/132 mM Cl^-

† Values at high K^+/20 mM Cl^- are significantly different from the values at high K^+/80 mM Cl^-

ANOVA,L.S.D.P<0.05

significant, an increase in $[K^+]_e$ from 4.7 to 9 mM did decrease the number of excitable fibers in EDL to 93%, which was further reduced to 87% at 11 mM K^+ (Fig. 3-11A). Reducing $[Cl^-]_e$ while $[K^+]_e$ was maintained at 11 mM improved the number of excitable fibers back to 97%. A further reduction to 20 mM Cl^- reduced the number to 91%. Upon the return to 4.7 mM K^+, 98% of fibers were excitable. A similar trend was observed in soleus, for the exception being that at 9 and 11 mM K^+ the number of excitable fibers were significantly reduced (Fig. 3-11B). In addition, reducing the Cl^- concentration to 20 mM further impaired excitability at 9 mM K^+.

HYPERKALEMIC PERIODIC PARALYSIS

The main aim of this study was to test if a reduction in G_{Cl} could alleviate paralytic symptoms. Results obtained from wildtype demonstrated a proof of principle, but needed to be tested in the HEPP model.

CONTRACTILITY

Mean peak tetanic force for HEPP (at 200 and 140 Hz) was 22.67 ± 1.12 N/cm^2 in EDL and 14.20 ± 1.72 N/cm^2 in soleus. At the physiological stimulation frequency of 90 Hz, mutant EDL force was 8.02 ± 0.76 N/cm^2, compared to 8.89 ± 2.88 N/cm^2 in wildtype EDL. In mutant soleus stimulated at its physiological level of 30 Hz, force was only 2.33 ± 0.83 N/cm^2, but was 7.28 ± 1.53 N/cm^2 in wildtype.

The effect of high $[K^+]_e$ was first tested at 8 mM K^+ in HEPP EDL, while stimulated at 90 Hz. This resulted in a non-significant shift in mean peak force to 112% (Fig. 3-12A), compared to a 160% potentiation in wildtype at 100 Hz (Fig. 3-6A). Another major difference was the variability among muscles at 8 mM K^+. Of the 3 HEPP EDL tested, 2 showed a potentiation in force while a third muscle showed a force depression; whereas

FIGURE 3-11

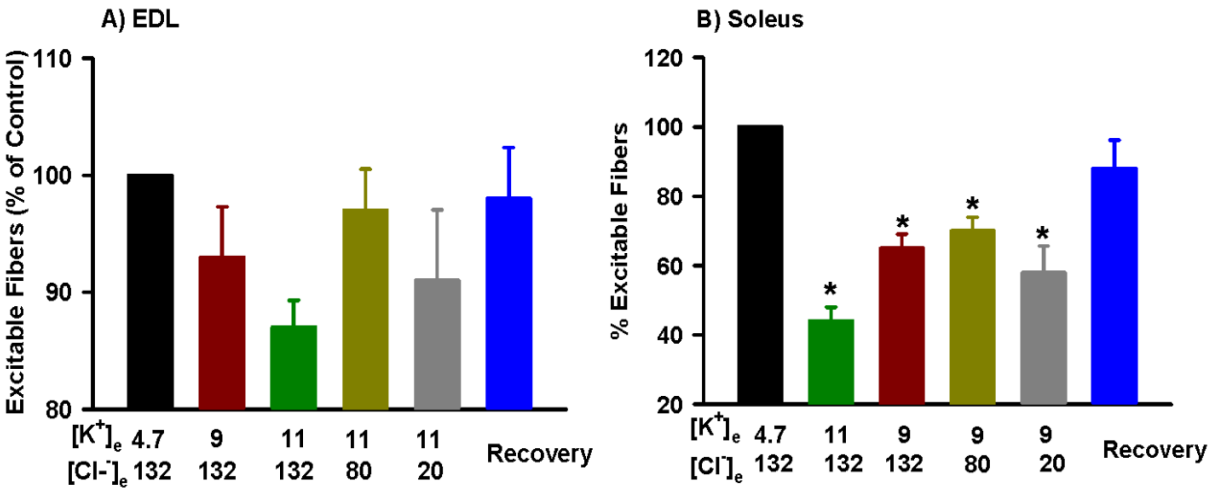

Figure 3-11. 80 mM Cl^- improved membrane excitability at high $[K^+]_e$ in A) EDL and B) soleus. Excitable fibers were fibers that elicited single action potentials upon stimulation. The number of excitable fibers is expressed as a % of the total number of fibers penetrated and stimulated to elicit action potentials. Vertical error bars represent S.E. for 5-8 muscles (for a total of 30-48 fibers at each condition).

* Significantly different from number of excitable fibers at 4.7 mM K^+

ANOVA, L.S.D. $P<0.05$

FIGURE 3-12

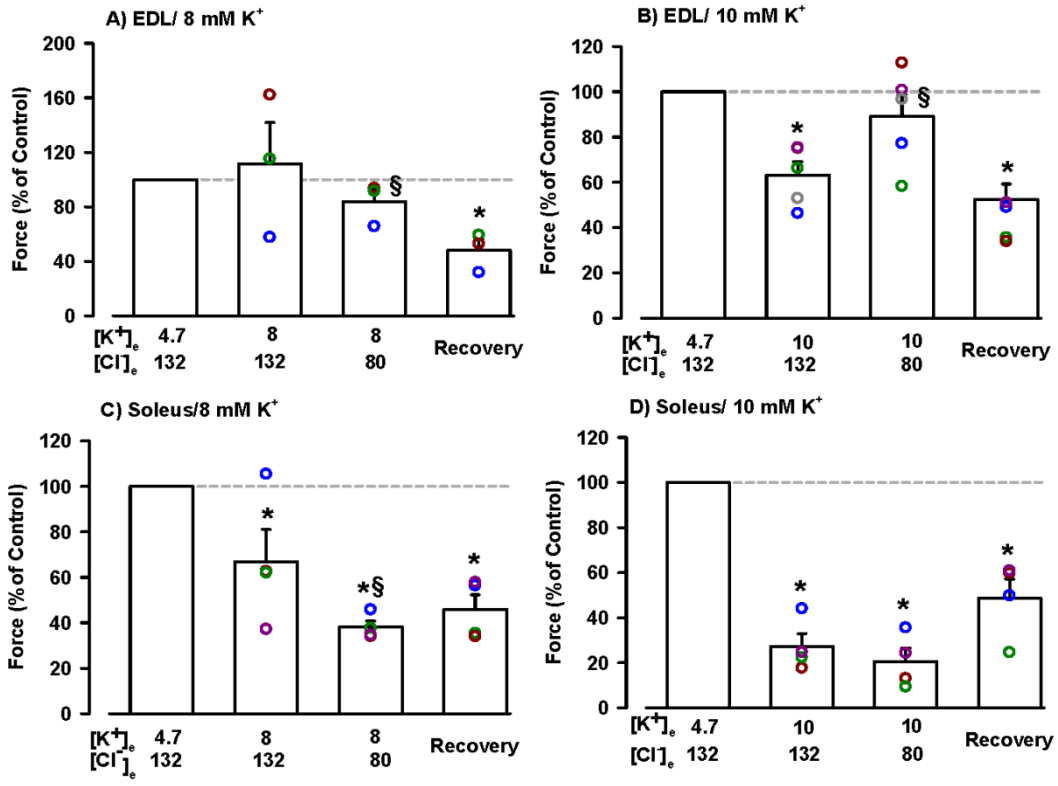

Figure 3-12. HEPP muscles exhibited large variability in responses to high $[K^+]_e$ and low $[Cl^-]_e$, which is characteristic of the disease. Responses in EDL to low Cl^- shown in A) at 8 mM K^+ and in B) at 10 mM K^+. C) and D) show soleus response under same conditions. EDL was stimulated at 90 Hz while soleus was stimulated at 30 Hz. A 2 sec train of pulses was provided every 10 min. Bars: mean peak force. Colored open circles: peak force from individual muscles. Peak forces are expressed as a percent of the force at 4.7 mM K^+ and 132 mM Cl^-. Vertical error bars represent S.E. for 3-5 muscles.

* Significantly different from mean peak force at 4.7 mM K^+

§ Mean peak force at high K^+/80 mM Cl^- is significantly different from that at high K^+/132 mM Cl^-

ANOVA, L.S.D. $P<0.05$

with wildtype EDL, a force depression at 90 Hz was never observed. At 10 mM K^+, the mean peak force decreased to 63% for HEPP EDL (Fig. 3-12B), while it enhanced force to 113% in wildtype EDL (Fig. 3-8A). HEPP soleus was stimulated at 30 Hz and an exposure to 8 mM K^+ caused a force depression to 67% (Fig. 3-12C) compared to a 150% potentiation in wildtype (Fig. 3-6B). Like EDL, 8 mM K^+ caused large variability in the force response of HEPP soleus as it potentiated force in one muscle to 105%, while it reduced force in the others to 40- 65%. The response to 10 mM K^+ was less variable then at 8 mM, as force further decreased to 27% (Fig. 3-12D), compared to a potentiation in wildtype to 174% (Fig. 3-8B). Thus, as previously reported, (Hayward *et al.*, 2007;Clausen *et al.*, 2011;Lucas *et al.*, 2014) HEPP muscles are more sensitive to the K^+-induced force depression than are wildtype muscles.

In most cases, reducing $[Cl^-]_e$ from 132 to 80 mM, while HEPP muscles were exposed to high $[K^+]_e$, did not increase force as observed in wildtype, i.e., most of the time a decrease in $[Cl^-]_e$ exacerbated the force decrease at high $[K^+]_e$. At 8 mM K^+, 80 mM Cl^- reduced mean HEPP EDL peak force from 112 to 84% (Fig. 3-12A). Even the two muscles that showed a force increase at 8 mM K^+ lost force when $[Cl^-]_e$ was reduced to 80 mM Cl^-. Interestingly, the other muscle that was depressed to 58% at 8 mM K^+ exhibited a small recovery in force to 66% upon reduction to 80 mM Cl^- (blue circle in Fig. 3-12A). At 10 mM K^+, 80 mM Cl^- significantly increased mean force in 4 out of 5 muscles, from a mean 63% to 89%; but reduced force in one muscle by 10% (green circle in Fig 3-12B). Thus, the response to high $[K^+]_e$ and low $[Cl^-]_e$ is highly variable between different HEPP EDL muscles.

The reduction to 80 mM Cl^- further reduced force at 8 mM K^+ in all tested HEPP

soleus muscles from a mean 67% to 38% (Fig. 3-12C). At 10 mM K^+, the reduction of Cl^- did not significantly affect force (Fig. 3-12D). Hence, a moderate reduction in $[Cl^-]_e$ was capable of improving force in only HEPP EDL muscles at 10 mM K^+, but not in HEPP soleus muscles.

Lastly, upon return to 4.7 mM K^+, force recovery back to 100% was either absent or significantly impaired. For both HEPP EDL and soleus muscles, force was only ~50% at the end of the 30 min recovery period. EDL, returning $[K^+]_e$ back to 4.7 mM at 132 mM Cl^- resulted in a further decrease in peak force to 50% (Fig. 3-12A,B). For HEPP soleus, there were slight recoveries in force from 38 to 46% for muscles that have been exposed to 8 mM K^+ (Fig. 3-12C) and from 21% to 49% for muscles exposed to 10 mM K^+ (Fig. 3-12D).

MEMBRANE EXCITABILITY

At 4.7 mM K^+, all wildtype EDL (30 fibers, 5 muscles) and soleus fibers (46 fibers, 8 muscles) generated normal action potentials with overshoots between 15-35 mV (Fig. 3-13A,B); while in HEPP, 5 out of 24 EDL fibers (20%, 3 muscles) and 5 out of 13 soleus fibers (38%, 2 muscles) had a reduced action potential overshoot between -25 and 14 mV (Fig. 3-13C,D). The remaining action potentials measured in HEPP muscle had an overshoot between -25 and 14 mV. Additionally, 8 out of 24 HEPP EDL fibers (33%) and 5 out of 13 HEPP soleus fibers (38%) exhibited myotonic discharge at 4.7 mM K^+ (Fig. 3-13E). Another abnormality observed solely in HEPP was a delayed onset of action potential after stimulation, although this was only observed in one EDL fiber and, as shown in Fig. 3-13F, in one soleus fiber. Overall, the mean resting E_M in HEPP muscles was 5-7 mV more depolarized compared to resting E_M for wildtype. At 4.7 mM

FIGURE 3-13

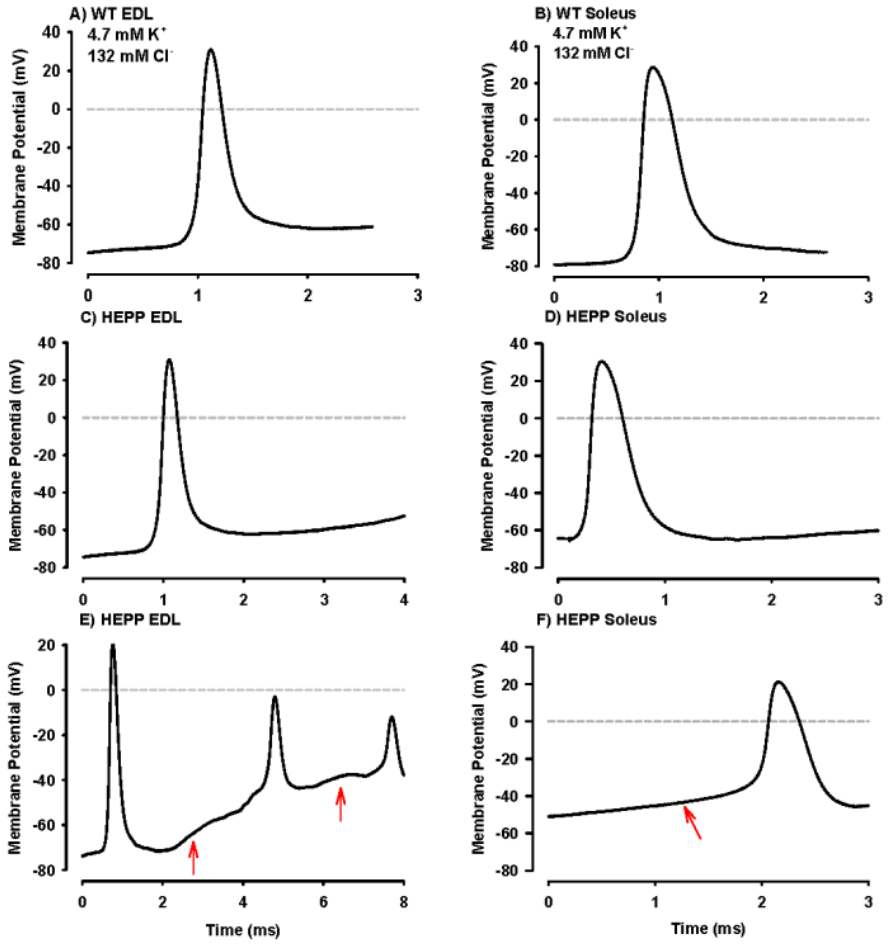

Figure 3-13. Representative single action potentials generated from wildtype and HEPP muscles at 4.7 mM K^+. A single stimulation was provided at time 0. Normal action potentials with an overshoot of 15-35 mV were generated in all wildtype fibers (A, B); in 19 of 24 HEPP EDL fibers (79%, 3 muscles) (C) and 8 of 13 HEPP soleus fibers (62%, 2 muscles). Remaining HEPP fibers showed a reduced overshoot between -25 and 14 mV. E) Example of myotonic discharge in HEPP EDL. Red arrow marks the second and third action potential generated in the absence of any electrical stimulation. F) Example of a delayed action potential after stimulation in HEPP soleus, indicated by a red arrow.

K^+, mean resting E_M of wildtype and HEPP EDL was -77 and -72 mV, respectively (Fig. 3-14A). For soleus, mean resting E_M were respectively -72 and -65 mV. On average, action potential overshoot was also depressed, to 18 mV for HEPP EDL and 15 mV for HEPP soleus (Fig. 3-14B).

Increasing $[K^+]_e$ from 4.7 to 10 mM in HEPP EDL (Fig. 3-15) resulted in a reduction in the number of excitable fibers to 60% (wildtype: 93% at 9 mM K^+, Fig. 3-11A), depolarized mean resting E_M to -58 mV (wildtype: -64 mV at 9 mM K^+, Fig.3-10A), and abolished action potential overshoot to from 18 to -8 mV (wildtype: 9 mV at 9 mM K^+, Fig. 3-10C). Reducing $[Cl^-]_e$ from 132 to 80 mM at 10 mM K^+ had no impact on resting E_M and action potential overshoot in HEPP and caused a slight decrease in the number of excitable fibers to 50%. Ten mM K^+ had a similar effect in HEPP soleus (Fig. 3-16), decreasing the amount of excitable fibers to 55% (wildtype: 65% at 9 mM K^+, Fig. 3-11B), depolarized resting E_M to -52 mV (wildtype: -59 mV at 9 mM K^+, Fig. 3-10B) and reduced action potential overshoot to -14 mV (wildtype: 8 mV at 9 mM K^+, Fig. 3-10D). Reducing Cl^- to 80 mM had no effect on resting E_M but slightly improved action potential overshoot to -10 mV. However, the number of excitable fibers was further reduced to 44%.

FIGURE 3-14

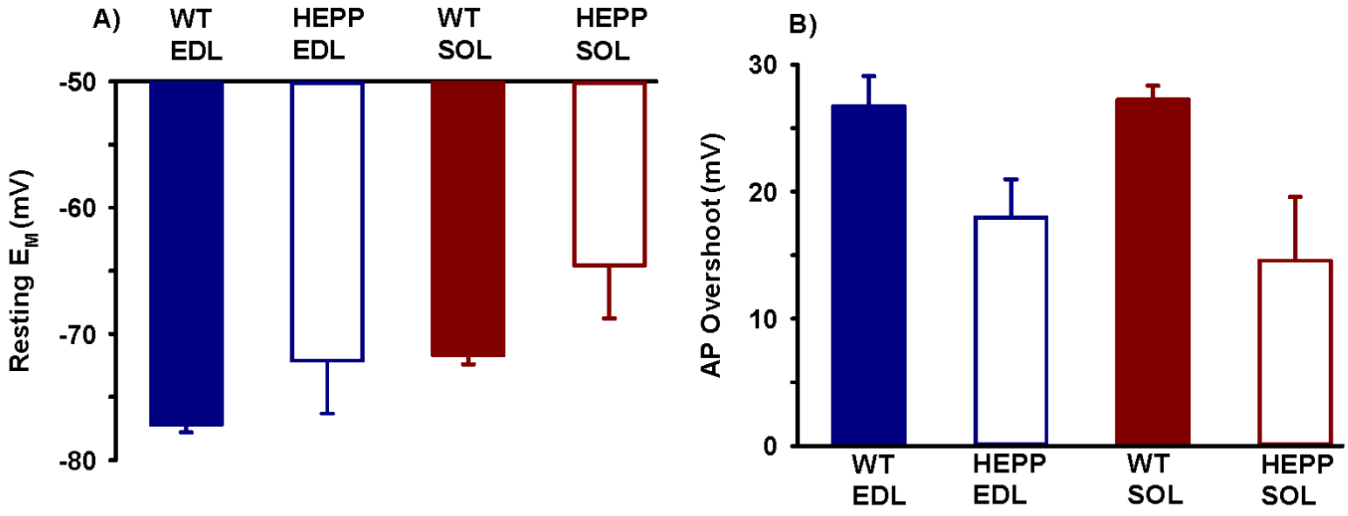

Figure 3-14. HEPP muscles have lower resting EM and action potential (AP) overshoot than those of wildtype muscles at 4.7 mM K^+. Vertical bar represents S.E. of 8 wildtype muscles (48 fibers in total) and 2-3 HEPP muscles (13-24 fibers in total).

FIGURE 3-15

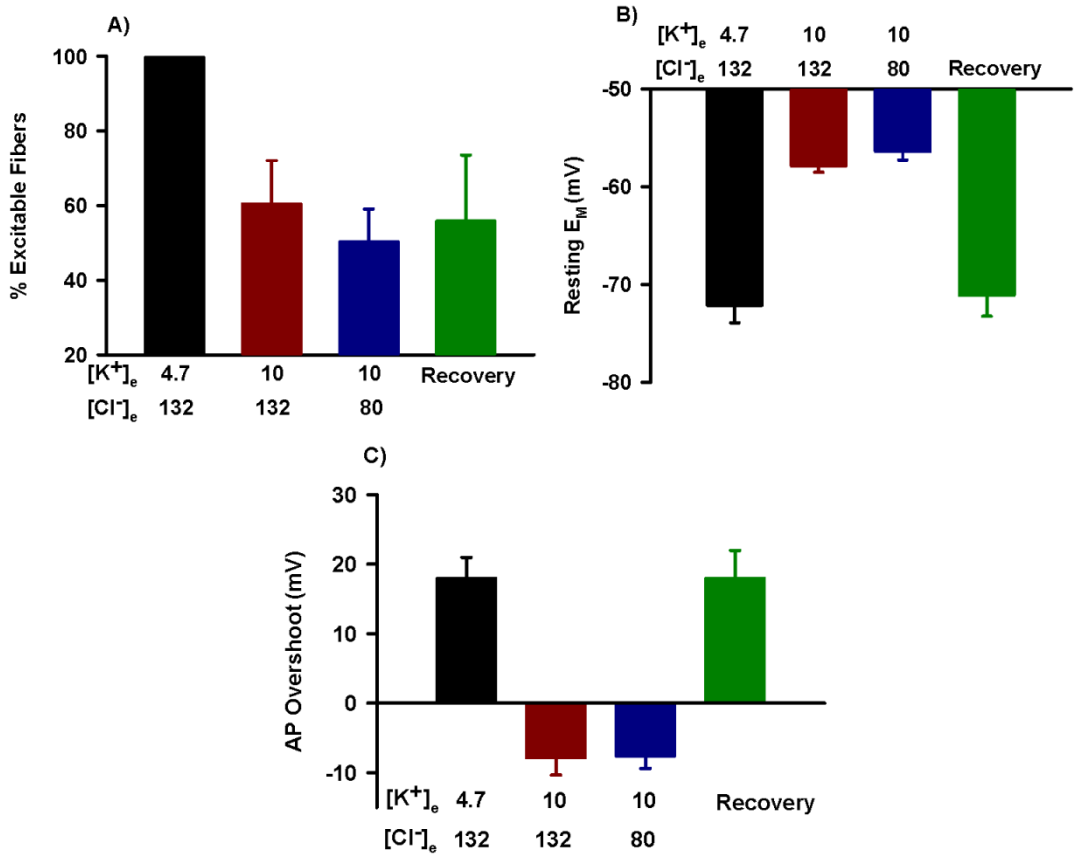

Figure 3-15. Eighty mM Cl^- had little impact on membrane potential properties in HEPP EDL. A) Number of excitable fibers was not increased at 10 mM K^+ when $[Cl^-]_e$ was reduced to 80 mM. B) The reduction in $[Cl^-]_e$ had no impact on resting E_M and C) action potential overshoot. Vertical bar represents S.E. of 3 muscles (15-25 fibers in total for each condition).

FIGURE 3-16

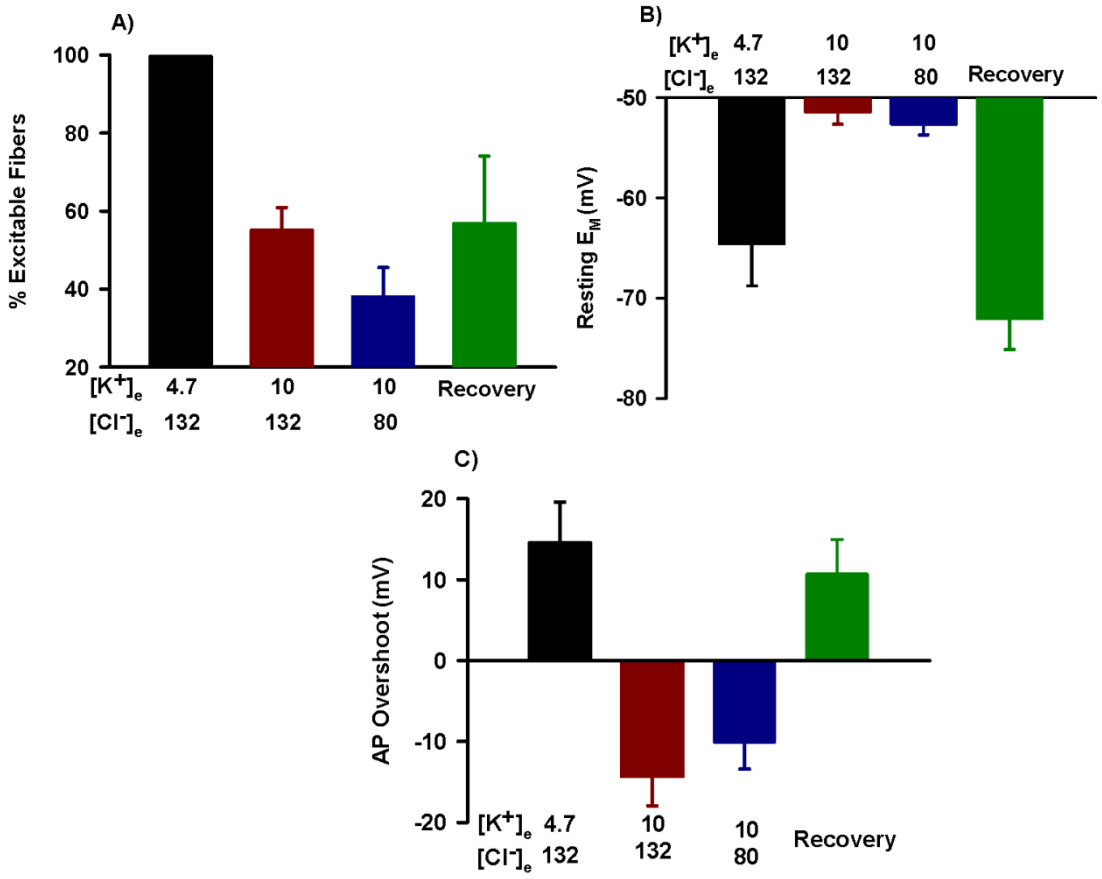

Figure 3-16. Eighty mM Cl^- had little impact on membrane potential properties in HEPP soleus. A) Number of excitable fibers was not increased at 10 mM K^+ when $[Cl^-]_e$ was reduced to 80 mM. B) The reduction in $[Cl^-]_e$ had no impact on resting E_M and C) action potential overshoot. Vertical bar represents S.E. of 2 muscles (13-17 fibers in total for each condition).

DISCUSSION

The major findings of this study at 37°C in wildtype are: 1) K^+-induced force potentiation force was not limited to twitch contraction as it also occurred at stimulation frequencies up to 50 Hz for soleus and 140 Hz for EDL; and 2) reduced G_{Cl} improved contractility at high $[K^+]_e$ and in some cases restored the K^+-induced force potentiation by improving membrane excitability, resting E_M and action potential overshoot.

The major findings in HEPP are that 1) contractile weakness in HEPP soleus, but not in HEPP EDL, was observed at 4.7 mM K^+ when stimulated at low frequencies; 2) force was depressed at lower $[K^+]_e$ compared to wildtype, due to severe depolarization of the resting E_M; 3) moderate reduction in $[Cl^-]_e$ at high $[K^+]_e$ improved force in some, but not all HEPP EDL muscles; and 4) low $[Cl^-]_e$ reduced fiber excitability and often depolarized resting E_M further to reduce action potential overshoot.

K^+ EFFECT IN WILDTYPE MUSCLES

K^+-INDUCED FORCE DEPRESSION

Increasing extracellular K^+ ($[K^+]_e$) from resting ~4.5 mM to 11 mM or higher is well known to depress membrane excitability (Hodgkin & Horowicz, 1959;Overgaard *et al.*, 1999). An increase in $[K^+]_e$ from 4.7 to 11 mM depolarized resting E_M by 43 mV for every 10-fold increase in $[K^+]_e$ for both EDL and soleus (Fig. 3-10). This value was much lower than the expected 61 mV depolarization calculated from the Nernst equation, but similar to values reported in a previous study (Yensen *et al*, 2002). As a consequence of the membrane depolarization, the action potential overshoot decreased. For example, from 4.7 at 11 mM K^+ action potential overshoot decreased from 20 to 5 mV (Fig. 3-10). The decrease in overshoot is a consequence of the Na_V channel slow-inactivation process.

It was therefore always thought that any increase in $[K^+]_e$ causes less Ca^{2+} release and force as action potential amplitude diminishes.

However, despite a 15 mV decrease in action potential overshoot at 11 mm K^+, EDL twitch force was not depressed until $[K^+]_e$ exceeded 13 mM, as previously reported (Yensen et al. 2002), while for the maximum tetanic force a depression was observed only when $[K^+]_e$ exceeded 11 mM. The same situation applies for soleus because its twitch and tetanic force became depressed when $[K^+]_e$ exceeded 10 and 8 mM, respectively, while action potential overshoot had decreased to 9 mV at 9 mM K^+. Thus, there is a range for which decreases in action potential overshoot does not lead to a reduction in force, in agreement with several previous studies (Yensen *et al.*, 2002;Cairns *et al.*, 2003;Pedersen *et al.*, 2003). The greater K^+-sensitivity of tetanic contraction compared to twitch contraction is also as previously reported in frog sartorius muscle and occurs because eventually muscle fibers do not generate an action potential to every stimulation during a tetanus preventing myoplasmic $[Ca^{2+}]$ to reach supra-maximal concentration (Renaud & Light, 1992).

The reported $[K^+]_e$ at which twitch and tetanic force depression occurs at 37°C in this study are much higher than those of other studies carried out strictly at lower temperatures; (Cairns *et al.*, 1997;Cairns *et al.*, 2003;Pedersen *et al.*, 2003) i.e., increases in temperature reduces the K^+ sensitivity by shifting the critical $[K^+]_e$ at which force is decreased to higher $[K^+]_e$. Only one comparative study has so far reported a greater K^+ sensitivity at 37°C than at 25°C (Cairns *et al.*, 2011), which may have been due to the accumulation of reactive oxygen species (ROS). A study by Van der Poel *et al.*, (2008) showed that a much larger ROS production occurred at 37°C compared to 25-32°C. They

incubated their muscles in vertical chambers with no superperfusion, allowing for ROS to accumulate. Under these conditions, muscle contractility was significantly reduced by 50%, an effect abolished by adding ROS scavengers. A similar setup was used in the study done by Cairns *et al*., (2011), which may explain why they observed greater force loss at 37°C compared to 25°C. In contrast, a study using a horizontal chamber with a superperfusion system at 15 ml/min showed that increasing $[K^+]_e$ to 10 mM decreased force in soleus 2-times more at 25°C than at 37°C (Lucas, 2012). More importantly, it was further shown that upon increasing temperature from 25°C to 37°C, while $[K^+]_e$ was at 10 mM, force increased to the amount generated from muscles kept at 37°C for the entire experiment. This suggests that the depressive effects of K^+ are more prevalent at 25°C compared to 37°C.

There are two mechanisms by which higher temperatures can alleviate the K^+-induced force depression. Firstly, when Na^+-K^+ ATPase (NKA) pumps are activated with ß-adrenergic agonist or insulin, peak force at 10 mM K^+ and 30°C increases back to its level at 4.7 mM K^+ (Clausen *et al.*, 1993).The same force increase at high $[K^+]_e$ occurs when temperature is increased instead of an activation by adrenergic agonist or insulin, unless ouabain, a specific NKA pump inhibitor is added (Pedersen *et al*,. 2003). As the NKA pump activity increases with temperature, it reduces the extent of the K^+-induced depolarization. In fact, this study and one by Yensen *et al.,* (2002) reported a smaller depolarization of 35-45 mV per 10-fold increase in $[K^+]_e$ at 37°C compared to 48-51 mV at 25°C (Cairns *et al*., 1997). The pump's repolarizing influence on the membrane potential is due to the fact that 3 Na^+ are pumped out while only 2 K^+ are pumped in, meaning that one positive charge is lost from the fiber during each cycle of the pump.

Secondly, increasing temperature causes a shift in the voltage dependence of slow inactivation to more depolarized potentials, which means that at a given E_M, the number of slow-inactivated Na_V channels is less at 37°C vs. 25°C. This reduction in inactivation allows for greater Na^+ current during the depolarization phase, resulting in greater action potential amplitude. Thus, the repolarizing effect of the NKA pumps as well as less slow-inactivation at 37°C act together to lower the K^+ sensitivity by maintaining a greater number of Na_V channels available for activation.

K^+-INDUCED FORCE POTENTIATION

Small increases in $[K^+]_e$ cause force potentiation. For twitch force, the potentiation at 8 mM K^+ was 75% in EDL and 55% in soleus (Fig-3.2). This potentiation is similar to that previously reported (Yensen et al. 2002) and is about 3-fold greater than the potentiation at 25°C (Cairns *et al.*, 1997). However, twitch and fused tetani are rare occurrences, as in vivo EDL and soleus are stimulated most commonly between 90-110 and 10-30 Hz, respectively (Hennig & Lomo, 1985). So, one major objective was to document whether the K^+-induced force potentiation also occurred at relevant stimulation frequencies. In this regard, a K^+-induced force potentiation was observed up to a frequency of 140 Hz in EDL and 50 Hz in soleus (Fig. 3-6). At these frequencies, tetani were unfused and thus muscles generated only submaximal force (Fig. 3-3). This meant that K^+ only potentiated force that was submaximal. EDL tetani fuse to generate maximal force at higher frequencies than in soleus and this explains why the K^+-induced force potentiation was observed at higher stimulation frequencies than in soleus. So, the K^+-induced force potentiation occurred at physiologically-relevant stimulation frequencies (see section "Physiological Relevance of the K^+ and Cl^- Effect" for further discussion on

this issue).

While the mechanism for the K^+-induced tetanic force depression is related to Na^+ channel inactivation as E_M depolarizes; the mechanism of the K^+-induced twitch potentiation is not well understood. It was recently reported though that a depolarization from -80 to -65 mV doubled the myoplasmic $[Ca^{2+}]$ ($[Ca^{2+}]_i$) at rest (Quinonez *et al.*, 2010). In fast-twitch fibers like EDL, such increases in $[Ca^{2+}]_i$ increases the amount of Ca^{2+} bound to Ca^{2+}-binding proteins, such as parvalbumin. Thus, when Ca^{2+} is released during subsequent contractions, more Ca^{2+} is available to troponin C, giving rise to greater activation of the sarcomere. In fact, $[Ca^{2+}]_i$ during a contraction increases when the membrane is depolarized to -70 mV, by injecting current or increasing $[K^+]_e$. The increase is due to either greater Ca^{2+} release from the SR or because Ca^{2+}-binding proteins are more saturated. Finally, it appears that $[Ca^{2+}]_i$ released during a contraction is influence by resting E_M because the Ca^{2+} transient following an action potential is the same at 2.5 and 10 mM K^+ when the resting E_M is clamped at -100 mV prior to the action potential. Thus the K^+-induced force potentiation may be due to a depolarization-induced elevation in free $[Ca^{2+}]_i$, resulting in an increased force generation.

EFFECT OF REDUCED Cl^- CONDUCTANCE ON CONTRACTILITY AT HIGH $[K^+]_e$

The reduction of Cl^- conductance (G_{Cl}) by lowering $[Cl^-]_e$ from 132 to 80 mM resulted in force recovery in K^+-depressed muscles (Fig. 3-7). This effect was largest at lower, physiologically-relevant stimulation frequencies (Hennig & Lomo. 1985) and became less effective as stimulation frequency increased. For example, at 13 mM K^+, 80 mM Cl^- improved EDL force by 65% at 90 Hz, but only by 30% at 150 Hz. This study also shows for the first time that the reduction in $[Cl^-]_e$ also augments force potentiation at

lower $[K^+]_e$ (Fig. 3-8). Further reduction in G_{Cl} by reducing $[Cl^-]_e$ to 20 mM, however, did not improve force recovery. It actually worsened the K^+ depression, which suggests an optimum G_{Cl}. This was confirmed by using 9-AC, assuming that the dose-response curve for the inhibition of ClC-1 channels in rat diaphragm is the same for mouse EDL and soleus (considering that they all express the ClC-1 isoform). If so, then a 70% decrease in G_{Cl} in EDL and 90% in soleus would be the optimal G_{Cl} for force recovery at high $[K^+]_e$.

An optimum G_{Cl} is in agreement with other studies. For rat soleus, an exposure to 11 mM K^+ reduced force (at 30 Hz) by 75%. When $[Cl^-]_e$ was reduced from 132 mM to 80 mM, force increased by 35% (Pedersen et al. 2005). While in another study, exposure to 9 mM K^+ reduced force by 20% and when $[Cl^-]_e$ was largely reduced from 130 mM to 10 mM, it resulted in another 40% decrease in force (Cairns *et al.*, 2004). The effect of reduced G_{Cl} was also previously tested on contractile endurance in soleus during a continuous 30 sec stimulating train which was examined at different $[Cl^-]_e$ (de Paoli *et al.*, 2013). At both 132 and 10 mM Cl^-, force first reached a peak in less than 1 sec and then continuously decayed to 40% of the peak value by the end of the 30 sec stimulation period. At 60 mM Cl^-, force only decayed to 65%. Overall, this study and others suggests that there is an optimal level of G_{Cl} reduction that improves force at high $[K^+]_e$ and during continuous stimulation (which causes an increase in $[K^+]_e$ in the t-tubules and interstitial space).

EFFECT OF CHLORIDE ON MEMBRANE POTENTIAL

As mentioned in the Introduction, Cl^- has opposing effects on membrane excitability. Cl^- stabilizes the resting membrane potential near -80 mV and reduces the extent of the K^+-induced membrane depolarization. The more the Cl^- conductance is

reduced, the greater the K^+ depolarization and thus the greater the K^+-induced force depression. Furthermore, Cl^- has an inhibitory or "shunting" influence on the depolarization phase of the action potential where it counteracts any depolarizing current to action potential threshold and the Na^+-induced depolarization phase. As G_{Cl} is reduced, the easier it is to get to threshold and the greater the action potential amplitude; both leading to more force at high $[K^+]_e$.

The beneficial effect on force upon reducing $[Cl^-]_e$ to 80 mM, or reducing G_{Cl} by 70%, was in part due to an improvement in the number of excitable fibers; i.e. the number of soleus fibers at 9 mM K^+ increased from 60 to 65%, while for EDL at 11 mM K^+ the increase was from 87 to 97% when $[Cl^-]_e$ was reduced from 132 to 80 mM (Fig. 3-11). It was also due to a hyperpolarization of resting E_M.

Interestingly, changing $[Cl^-]_e$ from 132 to 80 mM at high $[K^+]_e$ did not increase the extent

of depolarization as expected. Instead it hyperpolarized resting E_M by 1 to 2 mV in EDL and soleus (Fig. 3-10). This is in agreement with the reported hyperpolarizations of 2-3 mV upon reducing $[Cl^-]_e$ to 80 mM in other studies (van Emst *et al.*, 2004;Dulhunty, 1978;Aickin *et al.*, 1989). As a consequence of the hyperpolarization, there was a small 3-6 mV improvement in mean action potential overshoot in EDL at 11 mM K^+ and in soleus at 9 mM K^+ (Fig. 3-10). Although the 1 to 2 mV was not statistically significant, it is still physiologically important because, as shown by Cairns *et al*., (1997), the force-resting E_M relationship is quite steep with all force loss occurring over a narrow range of 5 mV. In this study, the small hyperpolarization shifted resting E_M away from the range that causes severe force loss. The question that arises then is how a reduction in $[Cl^-]_e$ to

80 mM results in hyperpolarization and not a depolarization as expected (as a large G_{Cl} normally opposes the K^+-induced membrane depolarization). The answer may involve the Na^+-K^+-$2Cl^-$ (NKCC1) transporter.

The secondary active transporter NKCC1 uses Na^+ for electrochemical energy to transport other ions into the cell against their electrochemical gradients, causing Cl^- to accumulate in the myoplasm (Betz *et al.*, 1984;Aickin *et al.*, 1989). As a consequence of this accumulation, there is a constant Cl^- efflux in the rest state that depolarizes the cell membrane. When $[Cl^-]_e$ is reduced to 80 mM, less Cl^- is transported because NKCC activity is reduced by mass action. This reduces both the electrochemical gradient of Cl^- and inward Cl^- current, contributing to a repolarization at high K^+ (Dulhunty, 1978). In other words, the hyperpolarization effect caused by lowering $[Cl^-]_e$ had a greater influence on E_M than the expected exacerbation of the K^+-induced depolarization.

Fig. 4-1 shows the relationship between resting E_M and overshoot obtained from the data at 4.7, 9 and 11 mM K^+ while Cl^- was left at 132 mM. When the data point for 11 mM K^+ and 80 mM Cl^- is plotted for EDL, it is slightly above the sigmoidal relationship from the K^+ data. For soleus, the data point appears directly on the sigmoidal curve. This demonstrates that for soleus, the increase in overshoot as $[Cl^-]_e$ is lowered to 80 mM is fully due to the hyperpolarization that reduces the level of Na^+ channel inactivation. In EDL, the slight increase above the sigmoidal relationship suggests that in addition to the hyperpolarizing effect, the lower Cl^- current during the Na^+-induced depolarization phase may also improve action potential amplitude. This effect may have been more apparent in EDL because it has a larger G_{Cl} than soleus (Pedersen *et al*., 2009).

Taken together, it is proposed that force improvement at high $[K^+]_e$ by a moderate

FIGURE 4-1

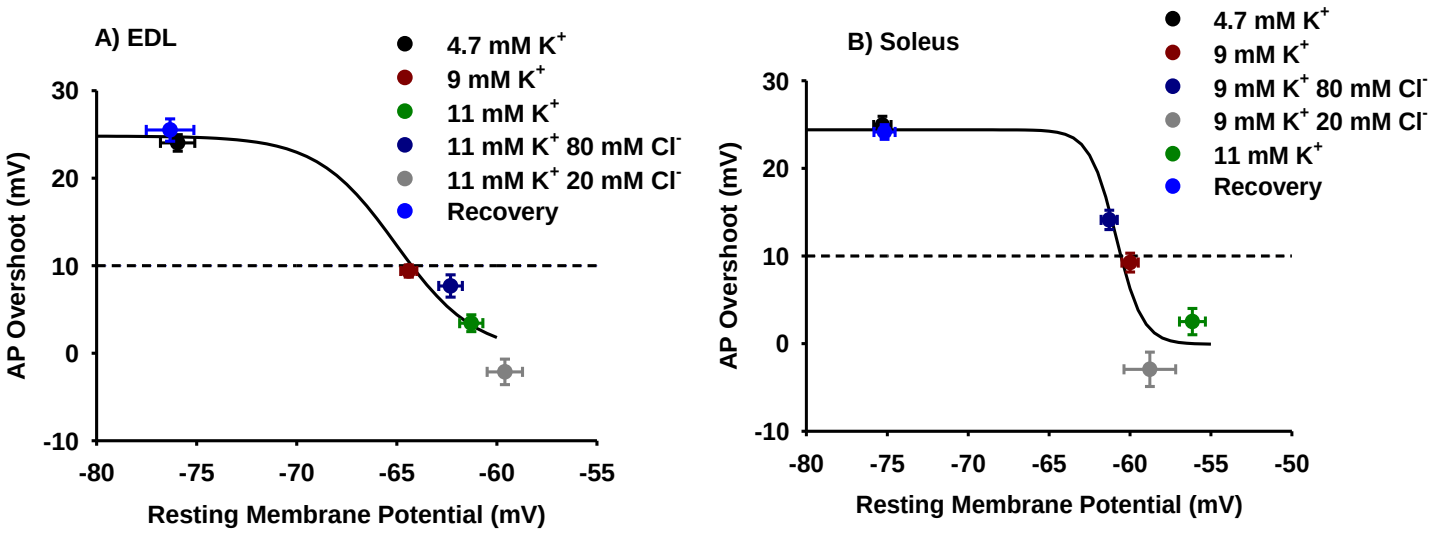

Figure 4-1. 80 mM Cl^- improved action potential overshoot by shifting resting E_M to a more negative potential. The black curves represent a fit from a sigmoidal curve using resting E_M and overshoot data from the measurement at 4.7, 9 and 11 mM K^+ while $[Cl^-]_e$ was kept at 132 mM. The data from 20 and 80 mM Cl^- are then plotted to determine if they fall on the sigmoidal curve. Vertical error bars represent the overshoot S.E. Horizontal bars represent the resting E_M S.E. Dashed line at 10 mV represents the critical overshoot at which lower action potential overshoot results in decreases in twitch force (Yensen *et al*., 2002). Number of samples is 24-48 fibers/ 5-8 EDL and 18-48 fibers/3-8 soleus.

reduction in G_{Cl} involves three factors: i) an increase in the number of excitable fibers; ii) a hyperpolarization that reduces the number of inactivated Na_V channels and iii) possibly a lower Cl^- current during the action potential depolarization phase, at least in EDL.

Further reduction in $[Cl^-]_e$ from 80 to 20 mM, or completely abolishing G_{Cl} with 100 µM 9-AC, exacerbated the K^+-induced force depression. This was associated with

further depolarization; e.g. EDL resting E_M at 11 mM K^+ and 20 mM Cl^- was less negative than at 11 mM K^+ with either 132 or 80 mM Cl^-. This is in agreement with previous studies that have shown greater depolarizations at high $[K^+]_e$ when Cl^- was reduced from 130 to 10 mM (Dulhunty, 1978;Cairns *et al.*, 2004). NKCC activity is most likely very low at 20 mM Cl^- and in the absence of Cl^- accumulation in the myoplasm, it eliminates the Cl^- current that depolarizes the membrane at rest. While blocking all Cl^- channels with 9-AC simply blocked the Cl^- depolarization. So, a greater K^+-induced depolarization occurs because the hyperpolarizing influence is lessened by the large reduction in $[Cl^-]_e$ to 20 mM. The larger depolarization subsequently reduces action potential overshoot (Fig. 4-1).

PHYSIOLOGICAL RELEVANCE OF THE K^+ AND Cl^- EFFECT

During a 30 min moderate 30 watt (W) leg exercise, interstitial $[K^+]$ measured within the quadriceps drastically increased from 4 mM to a mean value of 10 mM within 5 min (Nielsen *et al*., 2003). However, taking into account the standard deviation, K^+ rose up to 14 mM or more in some individuals. Considering that in this study K^+-induced force depression at 15 mM K^+ and 100 Hz in EDL was 88% complete, then a first question is "how did these individuals maintain the same workload when the $[K^+]_e$ was either close to or above the critical $[K^+]_e$ for force depression?". Furthermore, in the same study when the work load was incrementally increased until the point of fatigue (i.e. until the workload could no longer be maintained), mean interstitial $[K^+]_e$ was still ~10 mM. If K^+ contributes to the decrease in force during fatigue as suggested by several investigations (Bigland-Ritchie *et al.*, 1979;Clausen *et al.*, 2004;Sejersted & Sjogaard, 2000), then a second question is "how can $[K^+]_e$ be the same at the onset of exercise as

well as at the point of fatigue?". Finally, one can also ask a third question about the physiological importance of the K^+-induced force potentiation at lower $[K^+]_e$.

When EDL and soleus muscle fibers were stimulated with 0.3 msec pulses at 15 Hz for 3.5 sec repeatedly every 7 sec, G_{Cl} decreased by 70% within 5 min (Pedersen *et al.*, 2009).The reduction was mediated by protein kinase C (PKC), which phosphorylates ClC-1 Cl^- channels. The decrease in G_{Cl} at the onset of muscle activity can explain why a 30 W exercise can last 30 min despite high interstitial $[K^+]$. In fact, it can be suggested that the decrease in G_{Cl} is critical in preventing any K^+-induced force depression at the onset of exercise by shifting the K^+-force relationship towards higher $[K^+]_e$. More importantly, this study shows that the K^+-induced force potentiation at 12 mM in EDL (90 Hz) and 10 mM in soleus (30 Hz) was augmented by reducing Cl^- from 132 to 80 mM (Fig. 3-6). In the case of the soleus, force was actually enhanced by another 50% (Fig. 3-8). The protective effect of lowered G_{Cl} on the K^+-induced force potentiation can then have another beneficial effect.

When muscle must maintain a certain workload, such as the 30 W moderate exercise as described above, rather than an increase in contractile force or power, the force potentiation allows for the same amount of force to be produced at lower stimulation frequency. For example, as force potentiates at 8 mM K^+, a reduction in stimulation frequency from 100 Hz to 70 Hz in EDL and 30 Hz to 10 Hz in soleus would allow for a constant force to be generated. Any decreases in G_{Cl} may also help in further reducing stimulation frequency (Fig. 3-5). Interestingly, as humans produce multiple maximal voluntary contractions, the motor neurons do decrease their firing rates to muscle (Fuglevand & Keen, 2003). By reducing stimulation rate, (which for EDL over a

30 min period using 1 contraction per second) it means 54,000 less action potentials. The energy demand can be subsequently reduced because with less action potentials, less Ca^{2+} is released, reducing the ATP demand by the SR Ca^{2+} pump. Thus, the reduction in stimulation frequency may play a role in preserving energy and delaying the onset of fatigue, while maintaining constant force generation. One may argue that this may not be the case for a muscle like soleus, which is more K^+ sensitive. However, in vivo, Na^+ and K^+ fluxes are 6.5-fold lower in soleus than in EDL (Clausen *et al*., 2004), and if stimulated at lower frequencies, then the interstitial $[K^+]_e$ may not increase as much as 10-14 mM. Thus the force potentiation will then occur in soleus as well. Finally, K^+ is an important factor contributing to vasodilation, improving blood flow and oxygen delivery to active muscles (Clifford & Hellsten, 2004). So, the initial increase in interstitial $[K^+]$ is beneficial in improving muscle performance by reducing ATP consumption as stimulation frequency is reduced because of the force potentiation process. At the same time, it increases energy delivery by increasing blood flow. The question that remains is whether K^+ is a factor in the etiology of muscle fatigue.

Pedersen *et al*., (2009) reported a decrease in G_{Cl} at the onset of exercise, but over a long period of time they observed a 4-fold increase in G_{Cl} and 14-fold increase in G_K, the latter being due to the opening of K_{ATP} channels. The increase was observed only in EDL, which are composed of glycolytic and fatigable fibers and not in soleus, which are composed of oxidative and fatigue-resistant fibers (Banas *et al.*, 2011). Furthermore, onset of this response occurred earlier in EDL when incubated in glucose-free medium. Finally, it is well established that K_{ATP} channels are activated during an energy deficit. So the authors suggested that the increase in G_{Cl} and G_K is triggered by a metabolic stressor

that initiates fatigue, a process that protects the muscle from complete energy depletion and subsequent fiber damage (McKenna *et al.*, 2008). To date, there is no study showing that a large increase in G_{Cl} increases the K^+-induced force depression. We propose that it is more than likely that if a decrease in G_{Cl} diminishes the K^+-induced force depression, an increase in G_{Cl} will have the reverse effect. Furthermore, the increase in K_{ATP} channel activation is known to decrease force by directly reducing action potential amplitude (Matar *et al.*, 2001;Gong *et al.*, 2003). Thus the regulation of membrane excitability during muscle activity is complex and depends on at least the $[K^+]_e$, G_{Cl} and G_K. At the onset of activity, increases in $[K^+]_e$ maximize muscle performance, while the concomitant decrease in G_{Cl} prevents any K^+ force depression. When an energy crisis develops, increases in G_K, G_{Cl} and K^+ then reduces membrane excitability to reduce Ca^{2+} release and force to preserve ATP.

EFFECTS OF K^+ AND Cl^- IN HEPP MUSCLES

Experiments done in wildtype provides a proof of principle that an optimal reduction in Cl^- conductance alleviates the K^+-induced depressive effects as it increases the number of excitable fibers by repolarizing the resting membrane potential and improving action potential overshoot. The second aim of this study was to determine if a similar reduction in G_{Cl} could alleviate the extreme K^+ sensitivity of HEPP muscles. In a few cases it did, suggesting that there is a capacity for Cl^- to alleviate the K^+-induced force depression. However, in most cases, decreasing G_{Cl} exacerbated the force loss. Furthermore, once challenged with high $[K^+]_e$ and low G_{Cl}, most muscles failed to recover their initial force under control conditions. Thus, the level of G_{Cl} reduction may have proven to be too severe for HEPP.

CONTRACTILITY DEFECTS

HEPP EDL and soleus muscles generated similar amounts of tetanic force compared to that in wildtype at 4.7 mM K^+, with one exception. At 30 Hz, HEPP soleus generated 70% less force than wildtype. So far, previous studies have all reported that HEPP muscles produce less force than wildtype; with some studies reporting the EDL as being more affected (Hayward *et al.*, 2007;Lucas *et al.*, 2014), and others reporting the soleus to be the most affected (Clausen *et al*., 2011). Such variability in the contractile responses across all these studies is congruent with the disease in humans. Typically, HEPP symptoms are highly variable in terms of when paralysis occurs, with often normal strength between paralytic attacks. In one study, patients were found to produce normal hand grip strength, but a complete loss of force within 60 min after KCl ingestion (Wang & Clausen, 1976), which is the hallmark of the HEPP disease; i.e. a greater sensitivity to the K^+-induced force depression.

The results from this study were no exception. Here, the K^+ challenge was carried out not for the peak tetanic force (140-200 Hz) but at physiologically-relevant stimulation frequencies of 30 and 90 for soleus and EDL, respectively. Compared with wildtype, the critical $[K^+]_e$ for force depression was lower in HEPP, as several EDL and soleus muscles lost force at 8 mM (Fig. 3-12), a concentration that always caused potentiation in wildtype to 130% in EDL and 263% in soleus (Fig. 3-6). This is in agreement with all previous studies, which show that HEPP muscles from human patients and the M1592V mouse model have higher K^+ sensitivity than wildtype (Wang & Clausen, 1976;Clausen *et al.*, 1993;Clausen *et al.*, 2011;Hayward *et al.*, 2007). Although the sample size for membrane potential measurements was small in this study, E_M was more depolarized in HEPP than in WT muscles at 4.7 mM K^+, as previously reported (Clausen *et al.*, 2011)

and observed in this laboratory (Ammar & Renaud, *unpublished*). The same situation was also observed at high $[K^+]_e$. With the large depolarizations, action potential amplitudes in HEPP were more depressed (Fig. 4-2).

ACTION POTENTIAL ABNORMALITIES

This is the first study to measure action potentials from HEPP mouse muscle. Compared to wildtype, one-fifth of HEPP EDL and one-third of HEPP soleus (at 4.7 mM K^+) fibers had a reduced action potential overshoot below 15 mV. These action potential overshoots were smaller than the predicted overshoot for wildtype at the same resting E_M (Fig. 4-2). Since fast inactivation is not impaired, the reduced HEPP action potential overshoot cannot be explained by an increase in Na_V channel inactivation. Rather it may be due to a reduced Na^+ current during the action potential because the intracellular $[Na^+]$ of HEPP fibers is much higher than in normal fibers, due to the persistent Na^+ influx at rest (Lehmann-Horn *et al.*, 2007; Clausen et al. 2011). This reduces the Na^+ electrochemical gradient and thus the Na^+ influx during action potential generation. Two other abnormalities were observed in a few HEPP muscles, i.e. not all. Myotonic discharge, or the generation of multiple action potentials after the stimulation had ceased, was observed in one-third of HEPP EDL and soleus fibers (Fig. 3-13). The presence of of myotonia in HEPP is in agreement with previous electromyography (EMG) measurements that have shown that more than 50% of HEPP human patients had short bursts of myotonic discharge (Fournier *et al.*, 2004). The same is true in the HEPP mouse model in which myotonic discharge was easily triggered upon implanting the EMG electrodes into the muscle (Hayward *et al.*, 1997). Finally, increased EMG activity in HEPP mouse gastrocnemius was observed in situ (Dejong, 2012). The myotonia is due

FIGURE 4-2

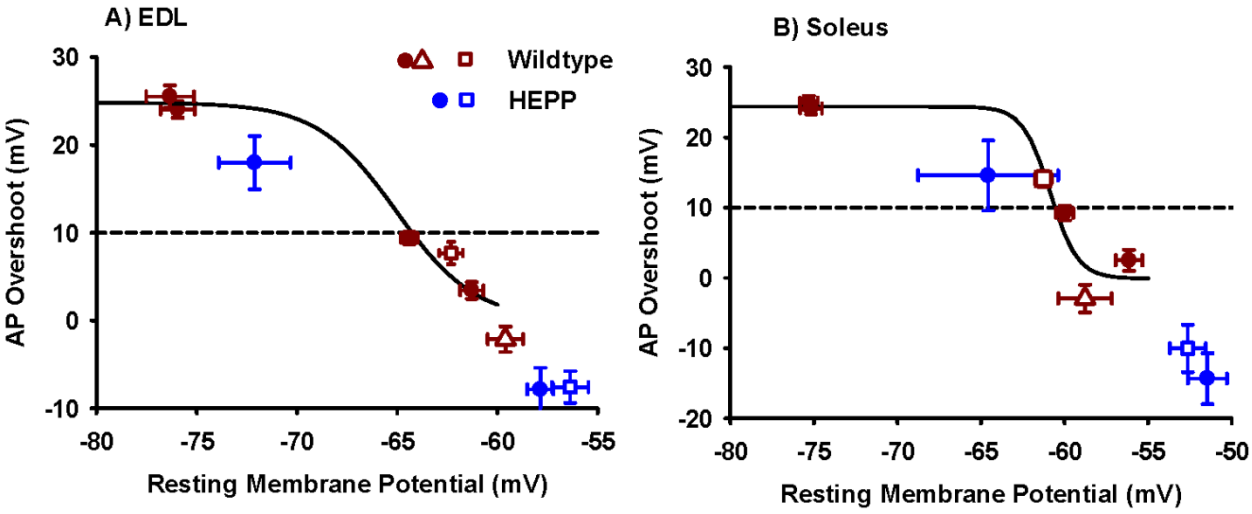

Figure 4-2. Resting E_M-Overshoot relationships for HEPP and wildtype. Same as Figure 4-1, but here it emphasizes the difference between wildtype and HEPP. Number of samples in HEPP is 24 fibers/3 EDL muscles and 13 fibers/ 2 soleus muscles.

Symbols: A) For WT, ● 4.7, 9, 11 mM K^+/132 mM Cl^-; □11 mM K^+ 80 mM Cl^-; Δ11 mM K^+ 20 mM Cl^-. For HEPP ● 4.7,10 mM K^+; □ 10 mM K^+/80 mM Cl^- B) Same except for WT, □ 9 mM K^+/80 mM Cl^-; Δ 9 mM K^+ 20 mM Cl^-.

to a depolarized resting E_M that is closer to action potential threshold, and due to less Na_V channel slow inactivation, making the generation of action potentials easier.

The other abnormality was only observed in a single HEPP EDL and soleus fiber, which was a very slow depolarization to threshold. This is likely caused by a decreased action potential propagation velocity. The presence of this abnormality would signal the onset of a paralytic attack, as it becomes more difficult for the fiber to generate action potentials. However, the fact that this abnormality was only observed in 2 muscle fibers reduces the significance of this finding.

Finally, the lack of recovery with reduced $[Cl^-]_e$ to 80 mM was associated with further depolarization while the same decrease in $[Cl^-]_e$ caused a hyperpolarization in wildtype. These two phenomena cannot be explained from the results of this study, but some possibilities can be proposed. One, resting E_M is already too unstable in HEPP and depending on the membrane state it can result in both a hyperpolarization and increased force as observed in very few fibers, or as observed for most fibers, a larger depolarization and force depression. While the reduction in G_{Cl} did improve action potential overshoot slightly in some HEPP soleus fibers (Fig. 3-16), this effect would have been greater if resting E_M was less depolarized. Two, NKCC pump or ClC-1 Cl^- channel activity may be different in HEPP than in wildtype so that E_{Cl}/E_M difference is not the same in HEPP compared to wildtype muscles. Three, the optimal G_{Cl} for force recovery in HEPP may be different than in wildtype muscles.

Decreases in G_{Cl} has the potential to improve force at high $[K^+]_e$ in HEPP muscles, but future studies will have to focus on 1) finding the optimal G_{Cl}; 2) using repolarizing agents such as pinacidil to activate K_{ATP} channels and salbutamol to activate

Na^+-K^+ ATPase pumps (in the attempt to stabilize resting E_M) prior to decreasing G_{Cl}; and 3) comparing expression levels of ClC-1 Cl- channels and NKCC1 between wildtype and HEPP.

CONCLUSION

In conclusion, this study has demonstrated that reducing G_{Cl} improves force generation at high $[K^+]_e$ at stimulation frequencies that naturally occur in vivo for mouse EDL and soleus. It was argued that this effect was critical for maximizing muscle performance at the onset of exercise. While the effect in wildtype muscles was a proof of principle that it can be explored for use to treat HEPP patients to reduce their high sensitivity to the K^+-induced force depression, this study demonstrated high variability in the Cl^- effect. In a few cases, lowering G_{Cl} at high $[K^+]_e$ did improve force generation, but in most cases it exacerbated the force depression. It is critical that following studies determine how the proportion of fibers for which a decrease in G_{Cl} improved force can be increased.

REFERENCES

Adrian RH & Bryant SH (1974). On the repetitive discharge in myotonic muscle fibres. *J Physiol* **240**, 505-515.

Aickin CC, Betz WJ, & Harris GL (1989). Intracellular chloride and the mechanism for its accumulation in rat lumbrical muscle. *J Physiol* **411**, 437-455.

Amin AS, Asghari-Roodsari A, & Tan HL (2010). Cardiac sodium channelopathies. *Pflugers Arch* **460**, 223-237.

Armstrong CM & Hille B (1998). Voltage-gated ion channels and electrical excitability. *Neuron* **20**, 371-380.

Banas K, Clow C, Jasmin BJ, & Renaud JM (2011). The K_{ATP} channel Kir6.2 subunit protein content is higher in glycolytic than in oxidative skeletel muscle fibers. *Am J Physiol* **301**, R916-R925.

Barclay CJ (2005). Modeling diffusive O_2 supply to isolated preparations of mammalian skeletal and cardiac muscle. *J Muscle Res Cell Motil* **26**, 225-235.

Begenisich TB & Cahalan MD (1980). Sodium channel permeation in squid axons. II: Non-independence and current-voltage relations. *J Physiol* **307**, 243-257.

Bendahhou S, Cummins TR, Tawil R, Waxman SG, & Ptacek LJ (1999). Activation and inactivation of the voltage-gated sodium channel: role of segment S5 revealed by a novel hyperkalaemic periodic paralysis mutation. *J Neurosci* **19**, 4762-4771.

Betz WJ, Caldwell JH, & Kinnamon SC (1984). Increased sodium conductance in the synaptic region of rat skeletal muscle fibres. *J Physiol* **352**, 189-202.

Bezanilla F & Armstrong CM (1977). Inactivation of the sodium channel. I. Sodium current experiments. *J Gen Physiol* **70**, 549-566.

Bigland-Ritchie B, Jones DA, & Woods JJ (1979). Excitation frequency and muscle fatigue: electrical responses during human volontary and stimulated contractions. *Exp Neurol* **64**, 414-427.

Brown DA & Adams PR (1980). Muscarinic suppression of a novel voltage-sensitive K+ current in a vertebrate neurone. *Nature* **283**, 673-676.

Cairns SP, Buller SJ, Loiselle DS, & Renaud JM (2003). Changes of action potentials and force at lowered [Na^+]o in mouse skeletal muscle: implication for fatigue. *Am J Physiol Cell Physiol* **285**, C1131-C1141.

Cairns SP, Hing WA, Slack JR, Mills RG, & Loiselle DS (1997). Different effects of raised [K^+]o on membrane potential and contraction in mouse fast- and slow-twitch muscle. *Am J Physiol* **273**, C598-C611.

Cairns SP, Leader JP, & Loiselle DS (2011). Exacerbated potassium-induced paralysis of mouse soleus muscle at 37°C vis-a-vis 25°C: implications for fatigue. *Pflugers Arch* **461**, 469-479.

Cairns SP, Ruzhynsky V, & Renaud JM (2004). Protective role of extracellular chloride in fatigue of isolated mammalian skeletal muscle. *Am J Physiol* **287**, C762-C770.

Campbell DT & Hahin R (1984). Altered sodium and gating current kinetics in frog skeletal muscle caused by low external pH. *J Gen Physiol* **84**, 771-788.

Cannon SC (2002). An expanding view for the molecular basis of familial periodic paralysis. *Neuromuscul Disord* **12**, 533-543.

Cannon SC (2006). Patomechanisms in channelopathies of skeletal muscle and brain. *Annu Rev Neurosci* **29**, 387-415.

Cannon SC, Brown RH, & Corey DP (1991). A sodium channel defect in hyperkalemic periodic paralysis: Potassium-induced failure of inactivation. *Neuron* **6**, 691-626.

Chang FC, Benton BJ, Salyer JL, Foster RE, & Franz DR (1990). Respiratory and cardiovascular effects of tetrodotoxin in urethane-anesthetized guinea pigs. *Brain Res* **528**, 259-268.

Clausen T, Andersen SLV, & Flatman JA (1993). Na^+-K^+ pump stimulation elicits recovery of contractility in K^+-paralysed rat muscle. *J Physiol (Lond)* **472**, 521-536.

Clausen T, Nielsen OB, Clausen JD, Pedersen TH, & Hayward LJ (2011). Na^+, K^+ pump stimulation improves contractility in isolated muscles of mice with hyperkalemic periodic paralysis. *J Gen Physiol* **138**, 117-130.

Clausen T, Nielsen OB, Harrison AP, Flatman JA, & Overgaard K (1998). The Na^+, K^+ - pump and muscle excitability. *Acta Physiol Scand* **162**, 183-190.

Clausen T, Overgaard K, & Nielsen OB (2004). Evidence that the Na^+ K^+ leak/pump ratio contributes to the difference in endurance between fast- and slow-twitch muscles. *Acta Physiol Scand* **180**, 209-216.

Clifford PS & Hellsten Y (2004). Vasodilatory mechanisms in contracting skeletal muscle. *J Appl Physiol (1985)* **97**, 393-403.

Cummins TR & Sigworth FJ (1996). Impaired slow inactivation in mutant sodium channels. *Biophys J* **71**, 227-236.

Cummins TR, Zhou J, Sigworth FJ, Ukomadu C, Stephan M, Ptácek LJ, & Agnew WS (1993). Functional consequences of a Na^+ channel mutation causing hyperkalemic perdiodic paralysis. *Neuron* **10**, 667-678.

Dejong, D (2012) Calcium alleviates symptoms in Hyperkalemic periodic paralysis by reducing the abnormal sodium influx. Master's thesis, University of Ottawa

de Paoli FV, Broch-Lips M, Pedersen TH, & Nielsen OB (2013). Relationship between membrane Cl- conductance and contractile endurance in isolated rat muscles. *J Physiol* **591**, 531-545.

de Paoli FV, Ortenblad N, Pedersen TH, Jorgensen R, & Nielsen OB (2010). Lactate per se improves the excitability of depolarized rat skeletal muscle by reducing the Cl- conductance. *J Physiol* **588**, 4785-4794.

Dirksen RT & Beam KG (1999). Role of calcium permeation in dihydropyridine receptor function. Insights into channel gating and excitation-contraction coupling. *J Gen Physiol* **114**, 393-403.

Dulhunty AF (1978). The dependence of membrane potential on extracellular chloride concentration in mammalian skeletal muscle fibres. *J Physiol (Lond)* **276**, 67-82.

Ebers GC, George AL, Barchi RL, Ting-Passador SS, Kallen RG, Lathrop GM, Beckmann JS, Hahn AF, Brown WF, Campbell RN, & Hudson AJ (1991). Paramyotonia congenita and hyperkalemic periodic paralysis are linked to the adult muscle sodium channel gene. *Ann Neurol* **30**, 810-816.

Edwards JN, Macdonald WA, van der Poel C, & Stephenson DG (2007). $O_2^{\cdot-}$ production at 37°C plays a critical role in depressing tetanic force of isolated rat and mouse skeletal muscle. *Am J Physiol* **293**, C650-C660.

Fahlke C, Rhodes TH, Desai RR, & George AL, Jr. (1998). Pore stoichiometry of a voltage-gated chloride channel. *Nature* **394**, 687-690.

Featherstone DE, Richmond JE, & Ruben PC (1996). Interaction between fast and slow inactivation in Skm1 sodium channels. *Biophys J* **71**, 3098-3109.

Fontaine B, Vale-Santos J, Jurkat-Rott K, Reboul J, Plassart E, Rime CS, Elbaz A, Heine R, Guimaraes J, Weissenbach J, & . (1994). Mapping of the hypokalaemic periodic paralysis (HypoPP) locus to chromosome 1q31-32 in three European families. *Nat Genet* **6**, 267-272.

Fournier E, Arzel M, Sternberg D, Vicart S, Laforet P, Eymard B, Willer JC, Tabti N, & Fontaine B (2004). Electromyography guides toward subgroups of mutations in muscle channelopathies. *Ann Neurol* **56**, 650-661.

Fuglevand AJ & Keen DA (2003). Re-evaluation of muscle wisdom in the human adductor pollicis using physiological rates of stimulation. *J Physiol* **549**, 865-875.

Gong B, Legault D, Miki T, Seino S, & Renaud JM (2003). K_{ATP} channels depress force by reducing action potential amplitude in mouse EDL and soleus. *Am J Physiol Cell Physiol* **285**, C1464-C1474.

Gordon AM, Homsher E, & Regnier M (2000). Regulation of contraction in striated muscle. *Physiol Rev* **80**, 853-924.

Green S, Bülow J, & Saltin B (1999). Microdialysis and the measurement of muscle interstitial K^+ during rest and exercise in humans. *J Appl Physiol* **87**, 460-464.

Green S, Langberg H, Skovgaard D, Bulow J, & Kjar M (2000). Interstitial and arterial-venous $[K^+]$ in human calf muscle during dynamic exercise: effect of ischaemia and relation to muscle pain. *J Physiol (Lond)* **529**, 849-861.

Hayward LJ, Brown RH, & Cannon SC (1997). Slow inactivation differs among mutant Na channels associated with myotonia and periodic paralysis. *Biophys J* **72**, 1204-1219.

Hayward LJ, Kim JS, Lee M-Y, Zhou H, Kim.J.W., Misra K, Salajegheh M, Wu F-F, Matsuda C, Reid V, Cros D, Hoffman EP, Renaud JM, Cannon SC, & Brown RH (2007). Targeted mutation of mouse $Na_V1.4$ muscle sodium channel produces myotonia and potassium-sensitive weakness. *J Clin Invest* **118**, 1437-1449.

Hennig R & Lomo T (1985). Firing patterns of motor units in normal rats. *Nature* **314**, 164-166.

Hilber K, Sandtner W, Zarrabi T, Zebedin E, Kudlacek O, Fozzard HA, & Todt H (2005). Selectivity filter residues contribute unequally to pore stabilization in voltage-gated sodium channels. *Biochemistry* **44**, 13874-13882.

Hodgkin AL & Horowicz P (1959). The influence of potassium and chloride ions on the membrane potential of single muscle fibres. *J Physiol (Lond)* **148**, 127-160.

Hodgkin AL & Huxley AF (1952). A quantitative description of membrane current and its application to conduction and excitation in nerve. *J Physiol (Lond)* **117**, 500-544.

Isom LL, De Jongh KS, & Catterall WA (1994). Auxiliary subunits of voltage-gated ion channels. *Neuron* **12**, 1183-1194.

Ji S, Sun W, George AL, Jr., Horn R, & Barchi RL (1994). Voltage-dependent regulation of modal gating in the rat SkM1 sodium channel expressed in Xenopus oocytes. *J Gen Physiol* **104**, 625-643.

Juel C, Bangsbo J, Graham T, & Saltin B (1990). Lactate and potassium fluxes from human skeletal muscle during and after intense, dynamic, knee extensor exercise. *Acta Physiol Scand* **140**, 147-159.

Juel C, Pilegaard H, Nielsen JJ, & Bangsbo J (2000). Interstitial K^+ in human skeletal muscle during and after dynamic graded exercise determined by microdialysis. *Am J Physiol* **278**, R400-R406.

Jurkat-Rott K & Lehmann-Horn F (2006). Paroxysmal muscle weakness - the familial peridoic paralyses. *J Neurol* **253**, 1391-1398.

Jurkat-Rott K & Lehmann-Horn F (2007a). Genotype-Phenotype correlation and therapeutic rationale in hyperkalemic peridoic paralysis. *Neurotherapeutics* **4**, 216-224.

Jurkat-Rott K & Lehmann-Horn F (2007b). Genotype-phenotype correlation and therapeutic rationale in hyperkalemic periodic paralysis. *Neurotherapeutics* **4**, 216-224.

Kontis KJ, Rounaghi A, & Goldin AL (1997). Sodium channel activation gating is affected by substitutions of voltage sensor positive charges in all four domains. *J Gen Physiol* **110**, 391-401.

Kristensen M, Hansen T, & Juel C (2004). Membrane proteins involved in potassium shifts during muscle activity and fatigue. *Am J Physiol* **290**, R766-R772.

Lehmann-Horn F (2004). Disease-causing mutations or functional polymorphisms? *Acta Myol* **23**, 85-89.

Lehmann-Horn F & Jurkat-Rott K (1999). Voltage-gated ion channels and hereditary disease. *Physiol Rev* **79**, 1317-1372.

Lehmann-Horn F, Rudel R, Ricker K, Lorkovic H, Dengler R, & Hopf HC (1983). Two cases of adynamia episodica hereditaria: in vitro investigation of muscle cell membrane and contraction parameters. *Muscle Nerve* **6**, 113-121.

Lucas B, Ammar T, Khogali S, DeJong D, Barbalinardo M, Nishi C, Hayward LJ, & Renaud JM (2014). Contractile abnormalities of mouse muscles expressing hyperkalemic periodic paralysis mutant NaV1.4 channels do not correlate with Na+ influx or channel content. *Physiol Genomics* **46**, 385-397.

Mallouk N & Allard B (2000). Streth-induced activation of Ca^{2+}-activated K^{+} channels in mouse skeletal muscle fibers. *Am J Physiol* **278**, C473-C479.

Matar W, Jasmin BJ, Lunde J, & Renaud JM (2001). Denervation enhances the effect of pinacidil and glibenclamide durng fatigue in EDL and soleus muscle. *Am J Physiol Cell Physiol*.

Matar W, Nosek TM, Wong D, & Renaud JM (2000). Pinacidil suppresses contractility and preserves energy but glibenclamide has no effect during fatigue in skeletal muscle. *Am J Physiol* **278**, C404-C416.

Matsuda H, Saigusa A, & Irisawa H (1987). Ohmic conductance through the inwardly rectifying K channel and blocking by internal Mg2+. *Nature* **325**, 156-159.

Matthews E, Fialho D, Tan SV, Venance SL, Cannon SC, Sternberg D, Fontaine B, Amato AA, Barohn RJ, Griggs RC, & Hanna MG (2010). The non-dystrophic myotonias: molecular pathogenesis, diagnosis and treatment. *Brain* **133**, 9-22.

McKenna MJ, Bangsbo J, & Renaud JM (2008). Muscle K+, Na+, and Cl– disturbances and Na+-K+ pump inactivation: implications for fatigue. *J Appl Physiol* **104**, 288-295.

Miller TC, da Silva D, Miller HA, Kwiecinski H, Mendell JR, Tawil R, McManis P, Griggs RC, Angelini C, Servidei S, Petajan J, Dalakas MC, Ranum LPW, Fu YH, & Ptácek LJ (2004). Correlating phenotype and genotype in the periodic paralyses. *Neurology* **63**, 1647-1655.

Ng JA, Vora T, Krishnamurthy V, & Chung SH (2008). Estimating the dielectric constant of the channel protein and pore. *Eur Biophys J* **37**, 213-222.

Nielsen JJ, Kristensen M, Hellsten Y, Bangsbo J, & Juel C (2002). Localization and function of ATP-sensitive potassium channels in human skeletal muscle. *Am J Physiol* **284**, R558-R563.

Nielsen JJ, Mohr M, Klarskov C, Kristensen M, Krustup P, Juel C, & Bangsbo J (2004). Effects of high-intensity intermittent training on potassium kinetics and performance in human skeletal muscle. *J Physiol (Lond)* **554**, 857-870.

Noda M, Shimizu S, Tanabe T, Takai T, Kayano T, Ikeda T, Takahashi H, Nakayama H, Kanaoka Y, Minamino N, & . (1984). Primary structure of Electrophorus electricus sodium channel deduced from cDNA sequence. *Nature* **312**, 121-127.

Overgaard K, Nielsen OB, Flatman JA, & Clausen T (1999). Relations between excitability and contractility in rat soleus muscle: role of the Na^+-K^+ pump and Na^+/K^+ gradients. *J Physiol (Lond)* **518**, 215-225.

Palade PT & Barchi RL (1977). Characteristics of the chloride conductance in muscle fibers of the rat diaphragm. *J Gen Physiol* **69**, 325-342.

Pearson CL (1964). The periodic paralyses: differential features and pathological observations in permanent myopathic weakness. *Brain* **87**, 341-354.

Pedersen TH, Clausen T, & Nielsen OB (2003). Loss of force induced by high extracellular [K^+] in rat muscle: effect of temperature, lactic acid and b_2-agonist. *J Physiol (Lond)* **551**, 277-286.

Pedersen TH, de Paoli F, & Nielsen OB (2005). Increased excitability of acidified skeletal muscle: role of chloride conductance. *J Gen Physiol* **125**, 237-246.

Pedersen TH, de Paoli FV, Flatman JA, & Nielsen OB (2009a). Regulation of CLC-1 and K_{ATP} channels in action potential-firing fast-twitch muscle fibers. *J Gen Physiol* **134**, 309-322.

Pedersen TH, Macdonald WA, de Paoli FV, Gurung.I.S., & Nielsen OB (2009b). Comparison of regulated passive membrane conductance in action potential-firing fast- and slow-twitch muscle. *J Gen Physiol* **134**, 323-337.

Plaster NM, Tawil R, Tristani-Firouzi M, Canún S, Bendahhou S, Tsunoda A, Donaldson MR, Iannaccone ST, Brunt E, Barohn R, Clark J, Deymeer F, George Jr. AL, Fish FA, Hahn A, Nitu A, Ozdemir C, Serdaroglu P, Subramony SH, Wolfe G, Fu Y-H, & Ptácek LJ (2001). Mutations in Kir2.1 cause the developmental and episodic electrical phenotypes of Andersen's syndrome. *Cell* **105**, 511-519.

Pusch M (2002). Myotonia caused by mutations in the muscle chloride channel gene CLCN1. *Hum Mutat* **19**, 423-434.

Quinonez M, Gonzalez F, Morgado-Valle C, & DiFranco M (2010). Effects of membrane depolarization and changes in extracellular [K(+)] on the Ca (2+) transients of fast skeletal muscle fibers. Implications for muscle fatigue. *J Muscle Res Cell Motil* **31**, 13-33.

Renaud JM & Light P (1992). Effects of K^+ on the twitch and tetanic contraction in the sartorius muscle of the frog, *Rana pipiens*. Implication for fatigue *in vivo*. *Can J Physiol Pharmacol* **70**, 1236-1246.

Sejersted OM & Sjogaard G (2000). Dynamics and consequences of potassium shifts in skeletal muscle and heart during exercise. *Physiol Rev* **80**, 1411-1481.

Street D, Nielsen JJ, Bangsbo J, & Juel C (2005). Metabolic alkalosis reduces exercise-induced acidosis and potassium accumulation in human skeletal muscle interstitium. *J Physiol (Lond)* **566**, 481-489.

Sun YM, Favre I, Schild L, & Moczydlowski E (1997). On the structural basis for size-selective permeation of organic cations through the voltage-gated sodium channel. Effect of alanine mutations at the DEKA locus on selectivity, inhibition by Ca2+ and H+, and molecular sieving. *J Gen Physiol* **110**, 693-715.

Terlau H, Heinemann SH, Stuhmer W, Pusch M, Conti F, Imoto K, & Numa S (1991). Mapping the site of block by tetrodotoxin and saxitoxin of sodium channel II. *FEBS Lett* **293**, 93-96.

Tikhonov DB & Zhorov BS (2007). Sodium channels: ionic model of slow inactivation and state-dependent drug binding. *Biophys J* **93**, 1557-1570.

van Emst MG, Klarenbeek S, Schot A, Plomp JJ, Doornenbal A, & Everts ME (2004). Reducing chloride conductance prevents hyperkalaemia-induced loss of twitch force in rat slow-twitch muscle. *J Physiol* **561**, 169-181.

Wang P & Clausen T (1976). Treatment of attacks in hyperkalemic familial periodic paralysis by inhalation of salbutamol. *Lancet* **307**, 221-223.

Wraight JM, Smith AD, Cowan JO, Flannery EM, Herbison GP, & Taylor DR (2004). Adverse effects of short-acting beta-agonists: potential impact when anti-inflammatory therapy is inadequate. *Respirology* **9**, 215-221.

Yang N, Ji S, Zhou M, Ptacek LJ, Barchi RL, Horn R, & George AL, Jr. (1994). Sodium channel mutations in paramyotonia congenita exhibit similar biophysical phenotypes in vitro. *Proc Natl Acad Sci U S A* **91**, 12785-12789.

Yensen C, Matar W, & Renaud JM (2002). The K^+-induced twitch potentiation is not due to longer action potential. *Am J Physiol* **283**, C169-C177.

Zhang Z, Xu Y, Dong PH, Sharma D, & Chiamvimonvat N (2003). A negatively charged residue in the outer mouth of rat sodium channel determines the gating kinetics of the channel. *Am J Physiol Cell Physiol* **284**, C1247-C1254.

Zhou Y, Morais-Cabral JH, Kaufman A, & MacKinnon R (2001). Chemistry of ion coordination and hydration revealed by a K+ channel-Fab complex at 2.0 A resolution. *Nature* **414**, 43-48.

Zimmer T (2010). Effects of tetrodotoxin on the mammalian cardiovascular system. *Mar Drugs* **8**, 741-762.